

**TABLE 1** Correlation between tumor-infiltrating CD204-positive macrophage density and clinicopathological features in patients with upper urinary tract cancer who underwent nephroureterectomy

| Clinical or pathologic feature | Total <i>N</i> | CD204 (tumor center) [ <i>n</i> (%)] |           | <i>p</i> value | CD204 (tumor periphery) [ <i>n</i> (%)] |         | <i>p</i> value |
|--------------------------------|----------------|--------------------------------------|-----------|----------------|---|---------|----------------|
|                                |                | Low                                  | High      |                | Low                                     | High    |                |
| All cases                      | 171            | 85 (50)                              | 86 (50)   |                | 85 (50)                                 | 86 (50) |                |
| Gender                         |                |                                      |           | 0.34           |   |         | 0.96           |
| Men                            | 119            | 62 (52)                              | 57 (48)   |                | 59 (50)                                 | 60 (50) |                |
| Women                          | 52             | 23 (44)                              | 29 (56)   |                | 26 (50)                                 | 26 (50) |                |
| Age (years)                    |                |                                      |           | 0.14           |   |         | 0.59           |
| <70                            | 93             | 51 (55)                              | 42 (45)   |                | 48 (52)                                 | 45 (48) |                |
| ≥70                            | 78             | 34 (44)                              | 44 (56)   |                | 37 (47)                                 | 41 (53) |                |
| Side                           |                |                                      |           | 0.25           |   |         | 0.82           |
| Left                           | 86             | 39 (45)                              | 47 (55)   |                | 42 (49)                                 | 44 (51) |                |
| Right                          | 85             | 46 (54)                              | 39 (46)   |                | 43 (51)                                 | 42 (49) |                |
| History of bladder cancer      |                |                                      |           | 0.81           |   |         | 0.81           |
| No                             | 140            | 69 (49)                              | 71 (51)   |                | 69 (49)                                 | 71 (51) |                |
| Yes                            | 31             | 16 (52)                              | 15 (48)   |                | 16 (52)                                 | 15 (48) |                |
| Tumor location                 |                |                                      |           | 0.03           |   |         | 0.23           |
| Renal pelvis                   | 103            | 58 (56)                              | 45 (44)   |                | 55 (53)                                 | 48 (47) |                |
| Ureter                         | 68             | 27 (40)                              | 41 (60)   |                | 30 (44)                                 | 38 (56) |                |
| Tumor architecture             |                |                                      |           | 0.0037         |   |         | 0.0037         |
| Papillary                      | 126            | 71 (56)                              | 55 (44)   |                | 71 (56)                                 | 55 (44) |                |
| Sessile                        | 45             | 14 (31)                              | 31 (69)   |                | 14 (31)                                 | 31 (69) |                |
| Grade                          |                |                                      |           | <0.0001        |   |         | <0.0001        |
| Low                            | 19             | 18 (95)                              | 1 (5.3)   |                | 19 (100)                                | 0       |                |
| High                           | 152            | 67 (44)                              | 85 (56 %) |                | 66 (43)                                 | 86 (57) |                |
| Lymphovascular invasion        |                |                                      |           | <0.0001        |   |         | <0.0001        |
| Absent                         | 97             | 61 (63)                              | 36 (37 %) |                | 62 (64)                                 | 35 (36) |                |
| Present                        | 74             | 24 (32)                              | 50 (68)   |                | 23 (31)                                 | 51 (69) |                |
| Concomitant carcinoma in situ  |                |                                      |           | 0.0046         |   |         | 0.0002         |
| Absent                         | 88             | 53 (60)                              | 35 (40)   |                | 56 (64)                                 | 32 (36) |                |
| Present                        | 83             | 32 (39)                              | 51 (61)   |                | 29 (35)                                 | 54 (65) |                |
| Tumor stage                    |                |                                      |           | <0.0001        |   |         | <0.0001        |
| pTa                            | 37             | 34 (92)                              | 3 (8.1)   |                | 35 (95)                                 | 2 (5.4) |                |
| pTis                           | 7              | 4 (57)                               | 3 (43)    |                | 3 (43)                                  | 4 (57)  |                |
| pT1                            | 31             | 17 (55)                              | 14 (45)   |                | 21 (68)                                 | 10 (32) |                |
| pT2                            | 18             | 8 (44)                               | 10 (56)   |                | 6 (33)                                  | 12 (67) |                |
| pT3                            | 69             | 22 (32)                              | 47 (68)   |                | 19 (28)                                 | 50 (72) |                |
| pT4                            | 9              | 0                                    | 9 (100)   |                | 1 (11)                                  | 8 (89)  |                |
| Lymph node metastasis          |                |                                      |           | 0.0017         |   |         | 0.0081         |
| Absent                         | 152            | 82 (54)                              | 70 (46)   |                | 81 (53)                                 | 71 (47) |                |
| Present                        | 19             | 3 (16)                               | 16 (84)   |                | 4 (21)                                  | 15 (79) |                |

significance of CD204<sup>+</sup> macrophages in renal cell carcinoma<sup>31</sup> or lymphoma.<sup>32</sup> In the present study, univariate and multivariate analysis show that tumor-infiltrating CD204<sup>+</sup> cell density associated significantly with shorter metastatic-free survival. Statistical significance was not achieved for cancer-specific survival in multivariate analysis, probably owing to fewer events and lower statistical power. Our

results suggest that tumor-infiltrating CD204<sup>+</sup> cell density may be a novel prognostic biomarker to predict metastasis in patients with upper urinary tract cancer.

To assess heterogeneity within a tumor, we evaluated two tissue cores taken from either the tumor center or the periphery for each case. While most previous studies on CD204 visually evaluated a few high-power

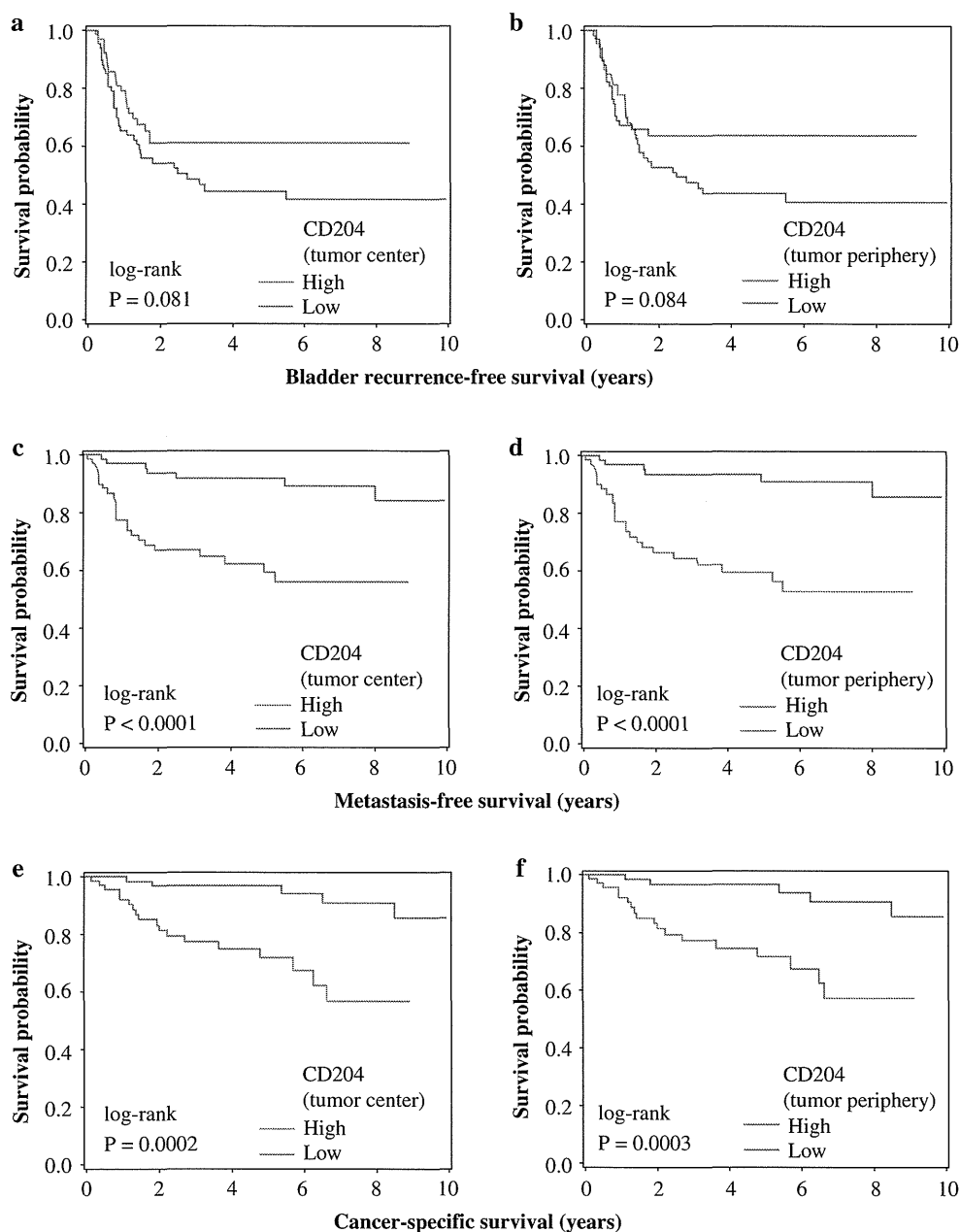


**FIG. 2** Kaplan–Meier analysis of bladder recurrence-free survival (**a, b**), metastasis-free survival (**c** and **d**), and cancer-specific survival (**e, f**) after nephroureterectomy according to CD204<sup>+</sup> macrophage density at the tumor center (**a, e**) and periphery (**b, f**). CD204<sup>+</sup> CD204-positive

fields,<sup>10–13,16,32,33</sup> here we evaluated CD204<sup>+</sup> cell density in a larger area (>6 mm<sup>2</sup> for each case) using validated image analysis software.<sup>21</sup> We found that CD204<sup>+</sup> cell density at the tumor center and the periphery strongly correlated, and that the associations of CD204 expression with clinicopathological features and patient outcomes were quite similar between them. Although further studies using whole slide sections are required to validate our findings,<sup>34,35</sup> our results suggest that CD204<sup>+</sup> cell density at either the tumor center or periphery may serve as a useful prognostic marker for upper urinary tract cancer.

Accumulating evidence suggests that tumor cells induce tumor-promoting CD204<sup>+</sup> macrophages to generate a specific microenvironment that supports tumor progression. Tumor-associated macrophages, which are recruited to tumors by multiple growth factors and chemokines that are often produced by tumor cells,<sup>8,36</sup> induce the proliferation, survival, and invasion of tumor cells by producing a wide range of factors, including matrix metalloproteinases and growth factors such as fibroblast growth factor and epidermal growth factor.<sup>37–39</sup> A recent study by Neyen et al.<sup>40</sup> shows that tumor progression and metastasis are inhibited

**TABLE 2** Tumor-infiltrating CD204-positive macrophage density in upper urinary tract cancer and patient outcomes (metastasis)

|  | Univariate analysis |                | Multivariate analysis |                |                  |                |
|--|---------------------|----------------|-----------------------|----------------|------------------|----------------|
|  | HR (95 % CI)        | <i>p</i> value | HR (95 % CI)          | <i>p</i> value | HR (95 % CI)     | <i>p</i> value |
| CD204 (tumor center) (high vs. low)                | 4.78 (2.06–11.1)    | 0.0003         | 2.52 (1.02–6.22)      | 0.045          | –                | –              |
| CD204 (tumor periphery) (high vs. low)             | 5.86 (2.40–14.3)    | 0.0001         | –                     | –              | 3.10 (1.17–8.16) | 0.022          |
| Sex (female vs. male)                              | 1.00 (0.46–2.17)    | 0.99           | –                     | –              | –                | –              |
| Age ( $\geq 70$ vs. $< 70$ years)                  | 2.03 (1.00–4.12)    | 0.050          | –                     | –              | –                | –              |
| Side (right vs. left)                              | 0.86 (0.43–1.72)    | 0.66           | –                     | –              | –                | –              |
| Tumor location (ureter vs. renal pelvis)           | 1.90 (0.95–3.80)    | 0.071          | –                     | –              | –                | –              |
| Tumor architecture (sessile vs. papillary)         | 1.57 (0.76–3.26)    | 0.23           | –                     | –              | –                | –              |
| Tumor grade (high vs. low) <sup>a</sup>            | –                   | –              | –                     | –              | –                | –              |
| Lymphovascular invasion (present vs. absent)       | 6.73 (2.90–15.6)    | $< 0.0001$     | 2.79 (1.02–7.65)      | 0.046          | 3.03 (1.08–8.49) | 0.035          |
| Concomitant carcinoma in situ (present vs. absent) | 3.16 (1.49–6.68)    | 0.0026         | –                     | –              | –                | –              |
| Tumor stage (pT2–pT4 vs. pTa–pT1)                  | 9.84 (2.99–32.4)    | 0.0002         | 2.69 (0.64–11.4)      | 0.18           | 1.89 (0.41–8.80) | 0.42           |
| Lymph node metastasis (present vs. absent)         | 6.37 (3.13–12.9)    | $< 0.0001$     | 2.30 (1.07–4.94)      | 0.034          | 2.64 (1.25–5.55) | 0.011          |
| Adjuvant chemotherapy                              | 2.87 (1.43–5.78)    | 0.0031         | –                     | –              | –                | –              |

The multivariate Cox regression models initially included CD204 status (tumor center or periphery), gender, age at diagnosis, tumor side, tumor location, tumor architecture, tumor grade, lymphovascular invasion, concomitant carcinoma in situ, tumor stage, lymph node metastasis, and adjuvant chemotherapy. A backward elimination was performed with a threshold of  $p = 0.05$ ; however, CD204 status, tumor stage, and lymph node metastasis were forced into the final models

CI confidence interval, HR hazard ratio

<sup>a</sup> Because patients with low-grade tumors did not experience an event, the hazard ratio could not be calculated

**TABLE 3** Tumor-infiltrating CD204-positive macrophage density in upper urinary tract cancer and patient outcomes (cancer-specific mortality)

|  | Univariate analysis |                | Multivariate analysis |                |                  |                |
|--|---------------------|----------------|-----------------------|----------------|------------------|----------------|
|  | HR (95 % CI)        | <i>p</i> value | HR (95 % CI)          | <i>p</i> value | HR (95 % CI)     | <i>p</i> value |
| CD204 (tumor center) (high vs. low)                | 5.41 (1.99–14.8)    | 0.001          | 2.75 (0.93–8.11)      | 0.067          | –                | –              |
| CD204 (tumor periphery) (high vs. low)             | 5.19 (1.91–14.1)    | 0.001          | –                     | –              | 2.50 (0.87–7.20) | 0.089          |
| Sex (female vs. male)                              | 0.98 (0.39–2.50)    | 0.97           | –                     | –              | –                | –              |
| Age ( $\geq 70$ vs. $< 70$ years)                  | 2.78 (1.19–6.52)    | 0.019          | –                     | –              | –                | –              |
| Side (right vs. left)                              | 0.84 (0.37–1.91)    | 0.67           | –                     | –              | –                | –              |
| Tumor location (ureter vs. renal pelvis)           | 1.50 (0.66–3.44)    | 0.34           | –                     | –              | –                | –              |
| Tumor architecture (sessile vs. papillary)         | 2.15 (0.94–4.91)    | 0.069          | –                     | –              | –                | –              |
| Tumor grade (high vs. low) <sup>a</sup>            | –                   | –              | –                     | –              | –                | –              |
| Lymphovascular invasion (present vs. absent)       | 13.4 (3.96–45.6)    | $< 0.0001$     | 5.15 (1.27–20.8)      | 0.022          | 5.24 (1.28–21.5) | 0.022          |
| Concomitant carcinoma in situ (present vs. absent) | 3.30 (1.36–8.03)    | 0.0085         | –                     | –              | –                | –              |
| Tumor stage (pT2–pT4 vs. pTa–pT1)                  | 22.7 (3.05–168.6)   | 0.0023         | 3.78 (0.38–37.7)      | 0.26           | 3.09 (0.28–33.7) | 0.35           |
| Lymph node metastasis (present vs. absent)         | 7.45 (3.26–17.0)    | $< 0.0001$     | 2.22 (0.92–5.35)      | 0.075          | 2.70 (1.15–6.32) | 0.022          |
| Adjuvant chemotherapy                              | 3.63 (1.54–8.57)    | 0.0033         | –                     | –              | –                | –              |

The multivariate Cox regression models initially included CD204 status (tumor center or periphery), gender, age at diagnosis, tumor side, tumor location, tumor architecture, tumor grade, lymphovascular invasion, concomitant carcinoma in situ, tumor stage, lymph node metastasis, and adjuvant chemotherapy. A backward elimination was performed with a threshold of  $p = 0.05$ ; however, CD204 status, tumor stage, and lymph node metastasis were forced into the final models

CI confidence interval, HR hazard ratio

<sup>a</sup> Because patients with low-grade tumors did not experience an event, the hazard ratio could not be calculated

in CD204-knockout mice in two in vivo models of ovarian and pancreatic cancer. Moreover, treatment of tumor-bearing mice with 4F, a small peptide ligand of CD204 that competes with physiological CD204 ligands, inhibited

tumor progression and metastasis.<sup>40</sup> Taken together, these observations suggest that tumor cells and CD204<sup>+</sup> macrophages may cooperate to contribute to more aggressive tumor behavior and that CD204 may be a potential drug

target in the prevention of metastatic cancer progression. Therefore, further studies on the crosstalk between urothelial cancer cells and CD204<sup>+</sup> macrophages are warranted.

Whereas CD204<sup>+</sup> cell density was associated with shorter metastasis-free and cancer-specific survival, it was not associated with bladder recurrence-free survival. It is likely that the ability of an upper urinary tract cancer to recur elsewhere in the urothelium may involve a different pathway. Whether other immune microenvironment markers such as lymphocyte surface antigens,<sup>41–44</sup> cytokines,<sup>45,46</sup> or chemokine receptors<sup>45</sup> can predict bladder recurrence is an important subject for future studies.

## CONCLUSIONS

Tumor-infiltrating CD204<sup>+</sup> cell density significantly associated with adverse prognostic factors and shorter metastatic-free and cancer-specific survival in patients with upper urinary tract cancer. Although further studies are required to validate our findings, our results suggest that a specific immune microenvironment may be associated with biological behavior of urothelial cancer and that CD204 may serve as a novel prognostic biomarker for these tumors.

**ACKNOWLEDGMENTS** This work was supported in part by a research grant from the Ichiro Kanehara Foundation for the Promotion of Medical Sciences and Medical Care (Teppei Morikawa), and a Grant-in-Aid for Scientific Research (C) from the Japan Society for the Promotion of Science (Teppei Morikawa). We are grateful to Yumiko Nagano, Harumi Yamamura, and Kei Sakuma for excellent technical support.

**CONFLICT OF INTEREST** Takashi Ichimura, Teppei Morikawa, Taketo Kawai, Tohru Nakagawa, Hirokazu Matsushita, Kazuhiro Kakimi, Haruki Kume, Shumpei Ishikawa, Yukio Homma, and Masashi Fukayama declare no conflicts of interest.

## REFERENCES

- Albini A, Sporn MB. The tumour microenvironment as a target for chemoprevention. *Nat Rev Cancer*. 2007;7(2):139–147.
- Wang T, Niki T, Goto A, et al. Hypoxia increases the motility of lung adenocarcinoma cell line A549 via activation of the epidermal growth factor receptor pathway. *Cancer Sci*. 2007;98(4):506–511.
- Matsubara D, Morikawa T, Goto A, Nakajima J, Fukayama M, Niki T. Subepithelial myofibroblast in lung adenocarcinoma: a histological indicator of excellent prognosis. *Mod Pathol*. 2009;22(6):776–785.
- Lu T, Gabrilovich DI. Molecular pathways: tumor-infiltrating myeloid cells and reactive oxygen species in regulation of tumor microenvironment. *Clin Cancer Res*. 2012;18(18):4877–4882.
- Rahir G, Moser M. Tumor microenvironment and lymphocyte infiltration. *Cancer Immunol Immunother*. 2012;61(6):751–759.
- Straussman R, Morikawa T, Shee K, et al. Tumour micro-environment elicits innate resistance to RAF inhibitors through HGF secretion. *Nature*. 2012;487(7408):500–504.
- Lewis CE, Pollard JW. Distinct role of macrophages in different tumor microenvironments. *Cancer Res*. 2006;66(2):605–612.
- Pollard JW. Tumour-educated macrophages promote tumour progression and metastasis. *Nat Rev Cancer*. 2004;4(1):71–78.
- Komohara Y, Ohnishi K, Kuratsu J, Takeya M. Possible involvement of the M2 anti-inflammatory macrophage phenotype in growth of human gliomas. *J Pathol*. 2008;216(1):15–24.
- Ohtaki Y, Ishii G, Nagai K, et al. Stromal macrophage expressing CD204 is associated with tumor aggressiveness in lung adenocarcinoma. *J Thorac Oncol*. 2010;5(10):1507–1515.
- Kurahara H, Shinchi H, Mataka Y, et al. Significance of M2-polarized tumor-associated macrophage in pancreatic cancer. *J Surg Res*. 2011;167(2):e211–219.
- Hirayama S, Ishii G, Nagai K, et al. Prognostic impact of CD204-positive macrophages in lung squamous cell carcinoma: possible contribution of Cd204-positive macrophages to the tumor-promoting microenvironment. *J Thorac Oncol*. 2012;7(12):1790–1797.
- Ito M, Ishii G, Nagai K, Maeda R, Nakano Y, Ochiai A. Prognostic impact of cancer-associated stromal cells in patients with stage I lung adenocarcinoma. *Chest*. 2012;142(1):151–158.
- Yoshikawa K, Mitsunaga S, Kinoshita T, et al. Impact of tumor-associated macrophages on invasive ductal carcinoma of the pancreas head. *Cancer Sci*. 2012;103(11):2012–2020.
- Ino Y, Yamazaki-Itoh R, Shimada K, et al. Immune cell infiltration as an indicator of the immune microenvironment of pancreatic cancer. *Br J Cancer*. 2013;108(4):914–923.
- Shigeoka M, Urakawa N, Nakamura T, et al. Tumor associated macrophage expressing CD204 is associated with tumor aggressiveness of esophageal squamous cell carcinoma. *Cancer Sci*. 2013;104(8):1112–1119.
- Grignon DJ. The current classification of urothelial neoplasms. *Mod Pathol*. 2009;22 Suppl 2:S60–69.
- Roupret M, Babjuk M, Comperat E, et al. European guidelines on upper tract urothelial carcinomas: 2013 update. *Eur Urol*. 2013;63(6):1059–1071.
- Morikawa T, Hino R, Uozaki H, et al. Expression of ribonucleotide reductase M2 subunit in gastric cancer and effects of RRM2 inhibition in vitro. *Hum Pathol*. 2010;41(12):1742–1748.
- Morikawa T, Sugiyama A, Kume H, et al. Identification of toll-like receptor 3 as a potential therapeutic target in clear cell renal cell carcinoma. *Clin Cancer Res*. 2007;13(19):5703–5709.
- Braun M, Kirsten R, Rupp NJ, et al. Quantification of protein expression in cells and cellular subcompartments on immunohistochemical sections using a computer supported image analysis system. *Histol Histopathol*. 2013;28(5):605–610.
- Miyata Y, Watanabe S, Kanetake H, Sakai H. Thrombospondin-1-derived 4N1 K peptide expression is negatively associated with malignant aggressiveness and prognosis in urothelial carcinoma of the upper urinary tract. *BMC Cancer*. 2012;12:372.
- Takeda T, Kikuchi E, Mikami S, et al. Prognostic role of KiSS-1 and possibility of therapeutic modality of metastatin, the final peptide of the KiSS-1 gene, in urothelial carcinoma. *Mol Cancer Ther*. 2012;11(4):853–863.
- Liang PI, Li WM, Wang YH, et al. HuR cytoplasmic expression is associated with increased cyclin A expression and poor outcome with upper urinary tract urothelial carcinoma. *BMC Cancer*. 2012;12:611.
- Miyazaki Y, Kosaka T, Mikami S, et al. The prognostic significance of vasohibin-1 expression in patients with upper urinary tract urothelial carcinoma. *Clin Cancer Res*. 2012;18(15):4145–4153.

26. Yoshimine S, Kikuchi E, Kosaka T, et al. Prognostic significance of Bcl-xL expression and efficacy of Bcl-xL targeting therapy in urothelial carcinoma. *Br J Cancer*. 2013;108(11):2312–2320.
27. Pignot G, Colin P, Zerbib M, et al. Influence of previous or synchronous bladder cancer on oncologic outcomes after radical nephroureterectomy for upper urinary tract urothelial carcinoma. *Urol Oncol*. 2014;32(1):23.e1-8.
28. Kitamura H, Torigoe T, Hirohashi Y, et al. Prognostic impact of the expression of ALDH1 and SOX2 in urothelial cancer of the upper urinary tract. *Mod Pathol*. 2013;26(1):117–124.
29. Chromecki TF, Bensalah K, Remzi M, et al. Prognostic factors for upper urinary tract urothelial carcinoma. *Nat Rev Urol*. 2011;8(8):440–447.
30. Lughezzani G, Burger M, Margulis V, et al. Prognostic factors in upper urinary tract urothelial carcinomas: a comprehensive review of the current literature. *Eur Urol*. 2012;62(1):100–114.
31. Komohara Y, Hasita H, Ohnishi K, et al. Macrophage infiltration and its prognostic relevance in clear cell renal cell carcinoma. *Cancer Sci*. 2011;102(7):1424–1431.
32. Komohara Y, Horlad H, Ohnishi K, et al. M2 macrophage/microglial cells induce activation of Stat3 in primary central nervous system lymphoma. *J Clin Exp Hematop*. 2011;51(2):93–99.
33. Nonomura N, Takayama H, Kawashima A, et al. Decreased infiltration of macrophage scavenger receptor-positive cells in initial negative biopsy specimens is correlated with positive repeat biopsies of the prostate. *Cancer Sci*. 2010;101(6):1570–1573.
34. Ogino S, Galon J, Fuchs CS, Dranoff G. Cancer immunology: analysis of host and tumor factors for personalized medicine. *Nat Rev Clin Oncol*. 2011;8(12):711–719.
35. Galon J, Franck P, Marincola FM, et al. Cancer classification using the Immunoscore: a worldwide task force. *J Transl Med*. 2012;10(1):205.
36. Hagemann T, Wilson J, Burke F, et al. Ovarian cancer cells polarize macrophages toward a tumor-associated phenotype. *J Immunol*. 2006;176(8):5023–5032.
37. Wyckoff J, Wang W, Lin EY, et al. A paracrine loop between tumor cells and macrophages is required for tumor cell migration in mammary tumors. *Cancer Res*. 2004;64(19):7022–7029.
38. Mantovani A, Allavena P, Sica A, Balkwill F. Cancer-related inflammation. *Nature*. 2008;454(7203):436–444.
39. Qian BZ, Pollard JW. Macrophage diversity enhances tumor progression and metastasis. *Cell*. 2010;141(1):39–51.
40. Neyen C, Pluddemann A, Mukhopadhyay S, et al. Macrophage scavenger receptor promotes tumor progression in murine models of ovarian and pancreatic cancer. *J Immunol*. 2013;190(7):3798–3805.
41. Gao Q, Zhou J, Wang XY, et al. Infiltrating memory/senescent T cell ratio predicts extrahepatic metastasis of hepatocellular carcinoma. *Ann Surg Oncol*. 2012;19(2):455–466.
42. Tsuchikawa T, Md MM, Yamamura Y, Shichinohe T, Hirano S, Kondo S. The immunological impact of neoadjuvant chemotherapy on the tumor microenvironment of esophageal squamous cell carcinoma. *Ann Surg Oncol*. 2012;19(5):1713–1719.
43. Katz SC, Bamboat ZM, Maker AV, et al. Regulatory T cell infiltration predicts outcome following resection of colorectal cancer liver metastases. *Ann Surg Oncol*. 2013;20(3):946–955.
44. Lee WS, Kang M, Baek JH, Lee JI, Ha SY. Clinical impact of tumor-infiltrating lymphocytes for survival in curatively resected stage IV colon cancer with isolated liver or lung metastasis. *Ann Surg Oncol*. 2013;20(2):697–702.
45. Yopp AC, Shia J, Butte JM, et al. CXCR4 expression predicts patient outcome and recurrence patterns after hepatic resection for colorectal liver metastases. *Ann Surg Oncol*. 2012;19 Suppl 3:S339–346.
46. Gu FM, Gao Q, Shi GM, et al. Intratumoral IL-17(+) cells and neutrophils show strong prognostic significance in intrahepatic cholangiocarcinoma. *Ann Surg Oncol*. 2012;19(8):2506–2514.

## ORIGINAL RESEARCH

# Intraperitoneal injection of in vitro expanded V $\gamma$ 9V $\delta$ 2 T cells together with zoledronate for the treatment of malignant ascites due to gastric cancer

Ikuo Wada<sup>1</sup>, Hirokazu Matsushita<sup>2</sup>, Shuichi Noji<sup>1</sup>, Kazuhiko Mori<sup>1</sup>, Hiroharu Yamashita<sup>1</sup>, Sachiyo Nomura<sup>1</sup>, Nobuyuki Shimizu<sup>1</sup>, Yasuyuki Seto<sup>1</sup> & Kazuhiro Kakimi<sup>2</sup>

<sup>1</sup>Department of Gastrointestinal Surgery, The University of Tokyo Hospital, Tokyo, Japan

<sup>2</sup>Department of Immunotherapeutics (Medinet), The University of Tokyo Hospital, Tokyo, Japan

## Keywords

Gastric cancer, malignant ascites, peritoneal dissemination, V $\gamma$ 9V $\delta$ 2 T-cell, zoledronate

## Correspondence

Kazuhiro Kakimi, Department of Immunotherapeutics, The University of Tokyo Hospital, 7-3-1 Hongo, Bunkyo-Ku, Tokyo 113-8655, Japan.  
Tel: 81-35805-3161; Fax: 81-35805-3164;  
E-mail: kakimi@m.u-tokyo.ac.jp

## Funding Information

This study was supported in part by a Grant-in-Aid for Scientific Research of the Ministry of Education, Culture, Sports, Science and Technology (K. K.).

Received: 17 October 2013; Revised: 28 November 2013; Accepted: 29 November 2013

*Cancer Medicine* 2014; 3(2): 362–375

doi: 10.1002/cam4.196

## Abstract

Malignant ascites caused by peritoneal dissemination of gastric cancer is chemotherapy-resistant and associated with poor prognosis. We conducted a pilot study to evaluate the safety of weekly intraperitoneal injections of in vitro expanded V $\gamma$ 9V $\delta$ 2 T cells together with zoledronate for the treatment of such malignant ascites. Patient peripheral blood mononuclear cells were stimulated with zoledronate (5  $\mu$ mol/L) and interleukin-2 (1000 IU/mL). After 14 days culture, V $\gamma$ 9V $\delta$ 2 T-cells were harvested and administered intraperitoneally in four weekly infusions. The day before T-cell injection, patients received zoledronate (1 mg) to sensitize their tumor cells to V $\gamma$ 9V $\delta$ 2 T-cell recognition. Seven patients were enrolled in this study. The number of V $\gamma$ 9V $\delta$ 2 T-cells in each injection ranged from 0.6 to 69.8  $\times 10^8$  (median 59.0  $\times 10^8$ ). There were no severe adverse events related to the therapy. Intraperitoneal injection of V $\gamma$ 9V $\delta$ 2 T cells allows them access to the tumor cells in the peritoneal cavity. The number of tumor cells in the ascites was significantly reduced even after the first round of therapy and remained substantially lower over the course of treatment. IFN- $\gamma$  was detected in the ascites on treatment. Computed tomography revealed a significant reduction in volume of ascites in two of seven patients. Thus, injection of these antitumor V $\gamma$ 9V $\delta$ 2 T-cells can result in local control of malignant ascites in patients for whom no standard therapy apart from paracentesis is available. Adoptively transferred V $\gamma$ 9V $\delta$ 2 T-cells do indeed recognize tumor cells and exert antitumor effector activity in vivo, when they access to the tumor cells.

## Introduction

Human T cells carrying  $\gamma\delta$  T-cell receptors account for 1–5% of peripheral blood T-cells [1, 2], the majority expressing the V $\gamma$ 9V $\delta$ 2 receptor [3] that recognizes phosphoantigens [4, 5]. Recently, much attention has been paid to V $\gamma$ 9V $\delta$ 2 T-cell-based cancer immunotherapy because these cells can secrete cytokines and exert potent cytotoxicity against a wide range of cancer cells [4]. Direct in vivo activation of V $\gamma$ 9V $\delta$ 2 T cells by nitrogen-containing bisphosphonates (NBPs) in cancer patients [6, 7] as well as adoptive transfer of ex vivo expanded

V $\gamma$ 9V $\delta$ 2 T cells have been investigated in several clinical trials [8, 9].

We have established a large-scale ex vivo expansion protocol for V $\gamma$ 9V $\delta$ 2 T cells using zoledronate and interleukin-2 (IL-2) [10, 11]. We found that such cultured T cells retained cytokine secretion capacity and mediated cytotoxicity against a variety of cancer cell lines [10]. On the basis of these findings, we conducted a clinical study in patients with advanced or recurrent non-small cell lung cancer resistant to standard therapy [12, 13]. The adoptive transfer of autologous V $\gamma$ 9V $\delta$ 2 T cells was well-tolerated. Some clinical benefit was observed in some

patients in whom V $\gamma$ 9V $\delta$ 2 T-cells were able to survive and expand, and in whom plasma IFN- $\gamma$  levels were elevated (but without statistical significance) [13]. However, it remained to be determined whether transferred V $\gamma$ 9V $\delta$ 2 T cells infiltrated into the tumor, recognized tumor cells and exerted antitumor effector functions *in vivo*. Therefore, we conducted a clinical study of intraperitoneal (i.p.) V $\gamma$ 9V $\delta$ 2 T-cell transfer therapy for the treatment of malignant ascites caused by peritoneal dissemination of gastric cancer.

Peritoneal dissemination is frequently observed in cases of advanced gastric cancer and occurs as a consequence of direct invasion and/or metastasis [14]. The presence of malignant ascites is a severe end-stage manifestation of the disease accompanied by several symptoms including nausea, appetite loss, abdominal tenderness and pain, fatigue and dyspnea, loss of proteins, and electrolyte disorders [15]. Recently, systemic chemotherapy with paclitaxel or S-1 plus cisplatin has improved the treatment of unresectable or recurrent gastric cancer [16–18]; i.p. chemotherapy [19] and immunotherapy, such as with catumaxomab [20], are also encouraging for the treatment of malignant ascites. However, to date, no options have been established for the management of peritoneal dissemination of ascites for patients' refractory to these treatments [15]. In such cases, only palliative therapies, such as paracentesis and diuretics, are available and the prognosis is extremely poor, with a median survival time of 3–4 months [21–23].

Therefore, we undertake adoptive cell therapy by injecting autologous V $\gamma$ 9V $\delta$ 2 T cells expanded *ex vivo* with zoledronate and IL-2 into the peritoneal cavity of patients with malignant ascites. Direct injection of these cells into the peritoneal cavity allows them access to the tumor cells, bypassing the difficulties of transferred V $\gamma$ 9V $\delta$ 2 T-cell recruitment into solid tumor. Because zoledronate leads to intracellular accumulation of isopentenyl pyrophosphate (IPP)/triphosphoric acid I-adenosine-50-yl ester 3-(3-methylbut-3-enyl) ester (A<sub>ppp</sub>I) in tumor cells that are then recognized by V $\gamma$ 9V $\delta$ 2 T cells by blocking the mevalonate pathway [24, 25], the injection of zoledronate preceded the infusion of expanded V $\gamma$ 9V $\delta$ 2 T-cells (Fig. 1). Using this approach, we asked the crucial question of whether zoledronate-expanded V $\gamma$ 9V $\delta$ 2 T-cells can recognize and kill tumor cells *in vivo*.

## Materials and Methods

### Study design and patient selection

This was a one-way, open-label, pilot study in patients with symptomatic malignant ascites secondary to gastric adenocarcinoma requiring symptomatic therapeutic

paracentesis. The primary objective of this study was to investigate the safety of i.p. injection of autologous V $\gamma$ 9V $\delta$ 2 T-cells. The secondary objectives were to obtain immunological proof-of-concept of antitumor activity of V $\gamma$ 9V $\delta$ 2 T-cells and to evaluate its clinical benefit. The research protocol was approved by the Ethical Committee of our institution (IRB-ID: P2010019-11Z), and registered at the University Hospital Medical Information Network Clinical Trials Registry (UMIN-CTR) (Unique trial number: UMIN000004130) on August 30, 2010. Written informed consent was obtained from each patient before they entered the study. The study was performed in accordance with the Declaration of Helsinki.

To be included, patients aged  $\geq 20$  years had to have histologically or cytologically proven gastric cancer, malignant ascites, an expected survival of at least 3 months, an Eastern Cooperative Oncology Group performance status (PS) of 0–2, normal kidney, liver, and bone marrow function, and be resistant to standard therapies. Patients positive for anti-adult T-cell leukemia-associated antigen or anti-human immunodeficiency virus antibody, other primary cancers, uncontrolled infection, active enterocolitis, severe heart disease, severe drug allergy, cryoglobulinemia, or autoimmune disease, were excluded from the study. Those receiving systemic steroid therapy or who were pregnant or lactating were also excluded. Small-scale 10-day V $\gamma$ 9V $\delta$ 2 T-cell culture screening tests were first performed to establish the reactivity of each patient's V $\gamma$ 9V $\delta$ 2 T cells prior to entry into the study. Proliferation was assessed as V $\gamma$ 9V $\delta$ 2 T-cell count on day 10 of culture/V $\gamma$ 9V $\delta$ 2 T-cell count at the initiation of culture. This value had to exceed 100 for the patient to be included in the study.

When the preliminary test fulfilled the criteria described above, leukapheresis was performed to isolate autologous peripheral blood mononuclear cells (PBMCs) and harvest plasma. Small-scale culture tests and leukapheresis were performed prior to chemotherapy; PBMCs and plasma were cryopreserved and stored before use. Patients received standard chemotherapy first; V $\gamma$ 9V $\delta$ 2 T-cell culture was initiated immediately when patients became resistant to the chemotherapy (Table 1). After 14 days culture, V $\gamma$ 9V $\delta$ 2 T-cells were harvested and administered i.p. to the patient. Four infusions were carried out weekly. The day before V $\gamma$ 9V $\delta$ 2 T-cell injection, patients received 1 mg of zoledronate (Novartis, Basel, Switzerland) (Fig. 1A). To ensure safety, zoledronate was administered intravenously (i.v.) on day 0 and i.p. via a catheter on days 7, 14, and 21 (Fig. 1B). Before each zoledronate or V $\gamma$ 9V $\delta$ 2 T-cell infusion and 1 day after cell infusion, blood (10 mL) was collected and ascites fluid (50 mL) was drained from the peritoneal cavity via the indwelling catheter for immunological analysis. When the

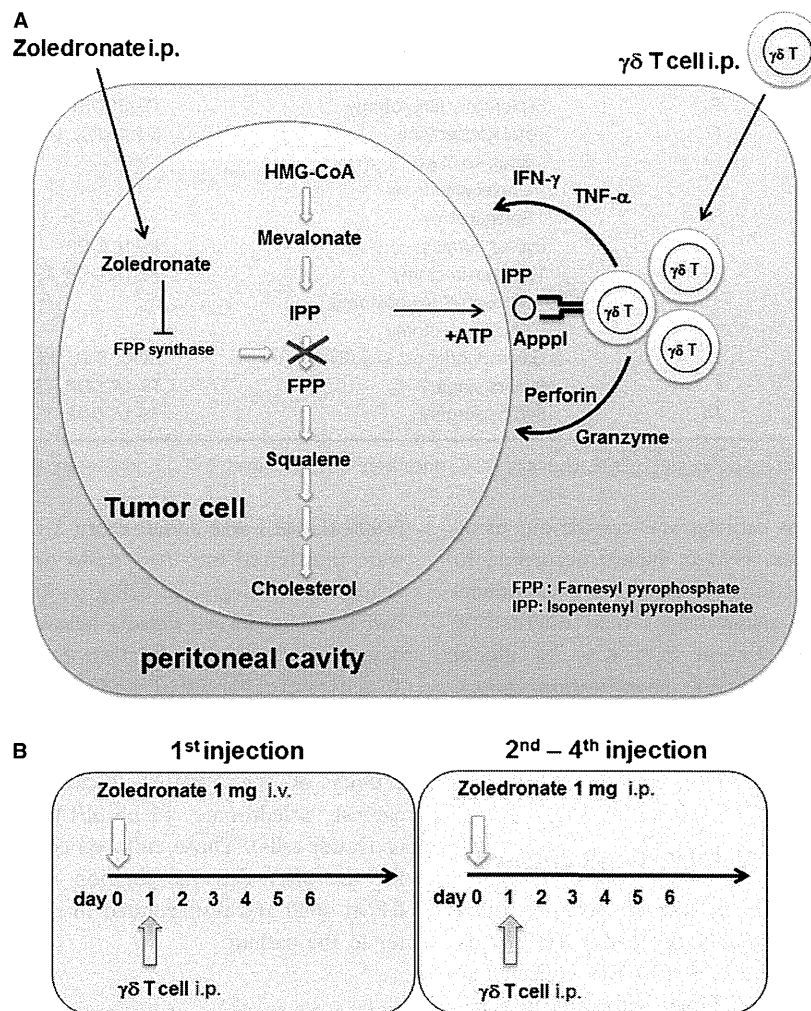


**Figure 1.** (A) Intraperitoneal administration of zoledronate sensitizes tumor cells to V $\gamma$ 9V $\delta$ 2 T-cell recognition. Isopentenyl pyrophosphate (IPP) is an intermediate metabolite in the mevalonate–cholesterol pathway, recognized by V $\gamma$ 9V $\delta$ 2 T-cells. Zoledronate inhibits farnesyl pyrophosphate (FPP) synthase, thereby causing the accumulation of IPP and triphosphoric acid l-adenosine-50-yl ester 3-(3-methylbut-3-enyl) ester (Apppl) in the tumor cells. When V $\gamma$ 9V $\delta$ 2 T-cells are injected into the peritoneal cavity, they can recognize IPP and respond to tumor cells. (B) The study scheme of weekly i.p. V $\gamma$ 9V $\delta$ 2 T-cell injection. In the first series of injections, zoledronate (1 mg) was administered i.v. on day 0, followed by i.p. V $\gamma$ 9V $\delta$ 2 T-cell injection on day 1. Zoledronate was i.p. injected via a catheter from the second to fourth injection.

patient experienced clinical benefit without significant toxicity, additional V $\gamma$ 9V $\delta$ 2 T-cell infusions were permitted.

**Safety assessment, antitumor effects, and quality of life**

Medical history, physical examination, PS, vital signs, chest X ray, electrocardiogram, and routine laboratory monitoring (including biochemistry, hematology, urinalysis, and tumor markers) were recorded at baseline. Thereafter, physical examination, PS, vital signs, and routine laboratory monitoring, as well as any adverse events, were assessed at each visit. Abdominal examination was

performed by the investigator to assess ascites signs, such as abdominal distension, dullness to percussion, shifting dullness, fluid thrill, and bulging flanks. Subjective symptoms related to ascites, such as anorexia, nausea, vomiting, abdominal pain, abdominal swelling, dyspnea, fatigue, and heartburn, were also recorded. Adverse events were graded according to National Cancer Institute–Common Terminology Criteria for Adverse Events version 4.0. Clinical responses were assessed by computed tomography performed at baseline and after the fourth infusion. To evaluate the antitumor effects of the treatment on peritoneal metastasis, the amount of malignant ascites and peritoneal cytology was also taken into account [26]. Cytology of ascites or peritoneal lavage fluid collected

**Table 1.** Summary of patients' background

| Patient ID | Age | Gender | Surgery  | Chemotherapy                          |
|------------|-----|--------|--|---------------------------------------|
| 2305       | 69  | F      | Exploratory laparotomy   | TS-1/CDDP, TS-1/DOC, CPT-11/CDDP, UFT |
| 2307       | 66  | F      | Total gastrectomy<br>Roux-en-Y jejunostomy<br>Cholecystectomy<br>Splenectomy | 5-FU/MTX, UFT, TS-1/CDDP, DOC         |
| 2319       | 58  | F      | Bypass surgery   | TS-1/CDDP                             |
| 2325       | 62  | M      | Total gastrectomy<br>Roux-en-Y jejunostomy<br>Cholecystectomy                | TS-1/CDDP, TS-1/DOC                   |
| 2334       | 39  | F      | Gastroduodenostomy (Billroth I)  | DOC, 5-FU+MTX, UFT, TS-1/CDDP         |
| 2336       | 47  | F      | Bypass surgery   | TS-1/CDDP, TS-1/PTX, CPT-11, PTX      |
| 2328       | 55  | M      | Bypass surgery   | TS-1/CDDP, TS-1/DOC                   |

TS-1, tegafur, gimeracil, and oteracil potassium; CDDP, cisplatin; DOC, docetaxel; PTX, paclitaxel; CPT-11, irinotecan; UFT, tegafur-uracil.

through a peritoneal access catheter was carried out using Diff-Quik staining (Sysmex, Hyogo, Japan) according to the manufacturer's instructions. The cellular components of ascites were evaluated using bright field microscopy (OLYMPUS BX41 with a Canon EOS Kiss X4 digital camera, OLYMPUS, Tokyo, Japan, magnification 200 $\times$ ). The safety assessment and clinical responses were determined by an independent data-monitoring committee after completion of the study.

### Isolation of PBMC and V $\gamma$ 9V $\delta$ 2 T-cell culture

V $\gamma$ 9V $\delta$ 2 T-cell culture was performed as previously described [10, 27, 28]. For small-scale 10-day V $\gamma$ 9V $\delta$ 2 T-cell culture tests, whole blood (7.5 mL) was collected in BD Vacutainer Cell Preparation Tubes with sodium heparin (Becton-Dickinson, Franklin Lakes, NJ) and directly centrifuged to isolate PBMC. To prepare V $\gamma$ 9V $\delta$ 2 T-cells for the therapy, patients underwent leukapheresis to isolate PBMC and harvest plasma using Fresenius AS.TEC204 with C4Y white blood cell set (FRESENIUS KABI, Bad Homburg, Germany). Sodium citrate (ACD-A solution; TERUMO, Tokyo, Japan) was used as the anticoagulant. PBMC and plasma were isolated by density gradient centrifugation using Lymphoprep (AXIS-SHIELD Poc AS, Oslo, Norway). Leukapheresis yielded more than  $1 \times 10^9$  PBMC and 100 mL plasma, both of which were cryopreserved until use. Depending on the data from small-scale 10-day V $\gamma$ 9V $\delta$ 2 T-cell culture tests, the number of PBMCs to set up large-scale V $\gamma$ 9V $\delta$ 2 T-cell cultures was estimated in order to obtain more than  $1 \times 10^9$  V $\gamma$ 9V $\delta$ 2 T-cells for each injection. PBMC were stimulated with 5  $\mu$ mol/L zoledronate in AlyS203 V $\gamma$ 9V $\delta$ 2 medium (Cell Science and Technology Institute, Sendai, Japan) containing 1000 IU/mL human recombinant IL-2 (Proleukin<sup>TM</sup>; Chiron, Amsterdam, The Netherlands), and 10% autologous plasma. Fresh medium containing IL-2

(1000 IU/mL) was added every 2–3 days and the cultures were transferred into new flasks or culture bags as necessitated by the degree of cell growth. Cultures were split in two to maintain cell density below  $1 \times 10^6$ /mL. Fourteen days after in vitro stimulation, ex vivo expanded V $\gamma$ 9V $\delta$ 2 T cells were harvested and screened for their sterility (negative for endotoxin, bacteria, fungus, and mycoplasma contamination) and purity (>60%). The cytotoxic activity of the V $\gamma$ 9V $\delta$ 2 T-cell cultures was evaluated against zoledronate (5  $\mu$ mol/L)-pretreated Daudi cells (z-Daudi cells). Those cultured cells which were approved for use after this examination were washed twice with RPMI-1640 and resuspended in normal saline to administer to the patient.

### Flow cytometry, immunofluorescence, and cytology

The following monoclonal antibodies (mAbs) were used for flow cytometry: FITC-labeled anti-CD3, -TCRV $\gamma$ 9, and -HLA-ABC, PE-labeled anti-TCR pan  $\alpha\beta$ , -NKG2D and mouse IgG<sub>1</sub> isotype, PC5-labeled anti-CD3, -CD8, -CD27, -CD56, and mouse IgG<sub>1</sub> isotype, ECD-labeled anti-CD4, -CD45, -CD45RA, and mouse IgG<sub>1</sub> isotype (Beckman Coulter, Immunotech, Marseille, France), PE-labeled anti-CD69 and -TCRV $\delta$ 2 (BD Bioscience Pharmingen, San Diego, CA), APC-labeled anti-EpCAM (Miltenyi Biotec, Bergisch Gladbach, Germany), and Pacific Blue-labeled anti-CD45 (BioLegend, San Diego, CA). Fixable Viability Dye eFluor 450 and 780 (eBioscience, San Diego, CA) were used to exclude dead cells. The cells were stained with antibodies and analyzed on a Cytomics FC 500 (Beckman Coulter) or Gallios (Beckman Coulter). The data were processed using Kaluza software (Beckman Coulter). Ascites cells were harvested by centrifugation and stained with mAbs described above. Tumor-cell load in ascites fluid (mL) was determined by

quantification of EpCAM<sup>+</sup> tumor cells in ascites fluid/peritoneal lavage. The cells were also resuspended in PBS and examined by confocal microscopy, FV10i (Olympus, Tokyo, Japan).

### Cytotoxicity assay

The cytotoxic activity of V $\gamma$ 9V $\delta$ 2 T-cells was examined by flow cytometry as described previously, with minor modifications [11, 29]. Daudi cells were obtained from the RIKEN BRC Cell Bank (Ibaraki, Japan) and grown in RPMI-1640 medium (Wako, Osaka, Japan) containing 10% fetal calf serum, streptomycin (100  $\mu$ g/mL), and penicillin (100 U/mL). Daudi cells were preincubated with 5  $\mu$ mol/L zoledronate overnight, resuspended in Diluent C (Sigma, St Louis, MO), and incubated for 2 min with 2  $\mu$ mol/L freshly prepared PKH-26 (Sigma) at room temperature. Daudi cells without zoledronate pretreatment were also used as target cells. After extensive washing, target cells were coincubated with effector cells at the indicated E/T ratio. After 1.5 h of *in vitro* incubation, cells in 0.1 mL of binding buffer (10 mmol/L HEPES, 140 mmol/L NaCl, 2 mmol/L CaCl<sub>2</sub>, pH 7.4) were incubated with 5  $\mu$ L of Annexin-V-FITC (BD Bioscience Pharmingen) and 20  $\mu$ g/mL of 7-aminoactinomycin D (7-AAD) (Sigma). Data analysis was performed first by gating on PKH-26-positive target cells followed by the analysis of Annexin-V-FITC- and 7-AAD-positive subpopulations. The percentage cytotoxicity in the PKH-26-gated cell population was calculated by subtracting the value of nonspecific Annexin-V-FITC- or 7-AAD-positive target cells, measured in appropriate controls without effector cells.

EpCAM<sup>+</sup> cells were enriched from ascites fluid using CD326 (EpCAM) Tumor Cell Enrichment and Detection Kit, human (Miltenyi Biotec) and stained with PKH-26 (Sigma). The labeled cells were plated on 35-mm glass bottom dish (Matsunami Glass Inc., Osaka, Japan) in RPMI-1640 medium containing 10% fetal calf serum with 5  $\mu$ mol/L zoledronate. V $\gamma$ 9V $\delta$ 2 T cells from same patient were expanded and labeled with 0.5  $\mu$ mol/L carboxyfluorescein diacetate succinimidyl ester (CFSE; Molecular Probes, Eugene, Oregon) according to the manufacturer's instructions. After EpCAM<sup>+</sup> cells adhered to the bottom of the dish, CFSE-labeled V $\gamma$ 9V $\delta$ 2 T-cells were added and cocultured under the confocal microscopy FV10i observation.

### CD107 translocation assay

Daudi cells were preincubated overnight with indicated concentration of zoledronate (0, 1, 5, 10, 50, and 100  $\mu$ mol/L, Novartis, Basel, Switzerland) to accumulate IPP or 10  $\mu$ mol/L pravastatin sodium (Cayman Chemical,

Ann Arbor, MI) to inhibit IPP synthesis. Zoledronate- or pravastatin-treated Daudi cells were used as stimulator cells and incubated with the same number of V $\gamma$ 9V $\delta$ 2 T-cells ( $5 \times 10^5$ ) for 2 h at 37°C in the presence of GolgiStop (BD bioscience), and anti-CD107a/b mAbs (BD bioscience). V $\gamma$ 9V $\delta$ 2 T cells were also stimulated with 20 ng/mL PMA/2  $\mu$ g/mL ionomycin (both from Sigma-Aldrich). Cells were then washed in PBS supplemented with 2% FCS, 1 mmol/L EDTA, and stained for 30 min at 4°C with anti-CD3 and -TCRV $\gamma$ 9. CD107 translocation was measured by flow cytometry.

### Cytokine measurement

Cytokines, including IL-1 $\beta$ , IL-2, IL-4, IL-5, IL-6, IL-8, IL-10, IL-12(p70), TNF- $\alpha$ , TNF- $\beta$ , and IFN- $\gamma$  in the plasma and ascites fluid were measured using FlowCytomix human Th1/Th2 11-plex kits (Bender MedSystems, Vienna, Austria) according to the manufacturer's instructions.

## Results

### Patients' characteristics

A total of seven patients underwent adoptive V $\gamma$ 9V $\delta$ 2 T-cell immunotherapy. The characteristics of the enrolled patients are summarized in Table 1. There were two men and five women with a median age of 58 years (range, 39–69). All patients had previously received surgery and chemotherapy. They were resistant to current possible standard chemotherapy, followed by 4-week washout period; then adoptive V $\gamma$ 9V $\delta$ 2 T-cell immunotherapy was reassessed. Malignant lesions were clinically restricted to the peritoneum in two cases (patients 2305 and 2319), while others had metastasized to lymph nodes, ovary, bladder, skin, and bones.

### Adoptive transfer of V $\gamma$ 9V $\delta$ 2 T cells

Aliquots of patients' PBMC were thawed and large-scale V $\gamma$ 9V $\delta$ 2 T-cell expansion cultures initiated 14 days prior to each injection. The number and percentage of V $\gamma$ 9V $\delta$ 2 T cells administered differed between individual patients and between separate infusions (Table 2). In most cases, the expansion of V $\gamma$ 9V $\delta$ 2 T cells from cryopreserved PBMCs was successful and  $>50 \times 10^8$  V $\gamma$ 9V $\delta$ 2 T cells were prepared for injections. However, the number of harvested V $\gamma$ 9V $\delta$ 2 T cells from the first large-scale culture was less than expected in patients 2305 and 2334, even though the number of cryopreserved PBMCs used was predetermined by the small-scale culture test. In these cases, more cryopreserved PBMCs were used for the next

large-scale expansion culture to ensure the availability of sufficient amounts of cells. The number of V $\gamma$ 9V $\delta$ 2 T cells in each injection ranged from 0.6 to  $69.8 \times 10^8$  (median  $59.0 \times 10^8$ ) (Table 2). The V $\gamma$ 9V $\delta$ 2 T cells from all of the patients displayed good effector function as assessed by their in vitro cytotoxicity against Daudi cells (Table 2).

Activated V $\gamma$ 9V $\delta$ 2 T cells exert antitumor effector activity through TCR and NK receptors such as NKG2D. NK receptors-dependent or V $\gamma$ 9V $\delta$ 2 TCR-dependent recognition of tumor cell was evaluated by CD107 translocation assay using pravastatin- or zoledronate-pretreated Daudi cells (Fig. 2). When the baseline tumor cell recognition by NK receptors was evaluated against pravastatin-treated Daudi cells, %CD107<sup>+</sup> V $\gamma$ 9V $\delta$ 2 T cells was 55%. The

proportion of CD107<sup>+</sup> V $\gamma$ 9V $\delta$ 2 T cells against Daudi or z-Daudi cells increased from 63.3% to 96.9% according to the concentration of zoledronate, and reached the plateau at 50  $\mu$ mol/L or higher. These results were consistent with previous reports that the optimum inhibition of FPP synthase activity was achieved by high zoledronate concentration [30]. The cytotoxic activities of patients' V $\gamma$ 9V $\delta$ 2 T cells against z-Duadi and Daudi cells were summarized in Table S2.

### Dynamics of zoledronate and V $\gamma$ 9V $\delta$ 2 T-cells injection

Three patients completed the course of four V $\gamma$ 9V $\delta$ 2 T-cell transfers; patient 2328 received an additional two

**Table 2.** Adoptively transferred V $\gamma$ 9V $\delta$ 2 T-cells

| Patient ID | Cell number ( $\times 10^8$ cells)<br>(purity of $\gamma\delta$ T cells) |              |              |              | Cumulative number<br>of $\gamma\delta$ T cell infusions<br>( $\times 10^8$ cells) | Average number of<br>$\gamma\delta$ T cell infusions<br>( $\times 10^8$ cells) | % cytotoxicity<br>against z-Daudi <sup>1</sup> E/T<br>ratio |      |      |
|------------|--|--------------|--------------|--------------|---|--|---|------|------|
|            | First  | Second       | Third        | Fourth       |   |  | 1:1   | 5:1  | 25:1 |
| 2305       | 0.6 (27.6%)  |              |              |              | 0.6   | 0.6  | 18.1  | 30.3 | 30.1 |
| 2307       | 58.8 (81.7%)   |              |              |              | 58.8  | 58.8   | 31.4  | 40.9 | 53   |
| 2319       | 55.4 (77.0%)   | 60.5 (84.0%) | 65.6 (85.2%) | 68.5 (85.6%) | 250   | 62.5   | 41.3  | 58   | 74.6 |
| 2325       | 49.7 (84.3%)   | 60 (88.3%)   | 69.8 (89.5%) | 40.1 (89.0%) | 219.6   | 54.9   | 14.2  | 39.3 | 60.2 |
| 2334       | 8.6 (71.5%)  | 45.1 (77.8%) | 52.7 (82.3%) |              | 106.4   | 35.5   | 45.1  | 79.7 | 84.6 |
| 2336       | 64.9 (94.0%)   |              |              |              | 64.9  | 64.9   | 28.9  | 57   | 55.4 |
| 2328       | 62.4 (90.4%)   | 59.2 (92.5%) | 65.7 (93.9%) | 51.7 (92.3%) | 239   | 59.8   | 38.3  | 64.5 | 72.2 |

<sup>1</sup>% cytotoxicity against Daudi cells was provided in Table S2.

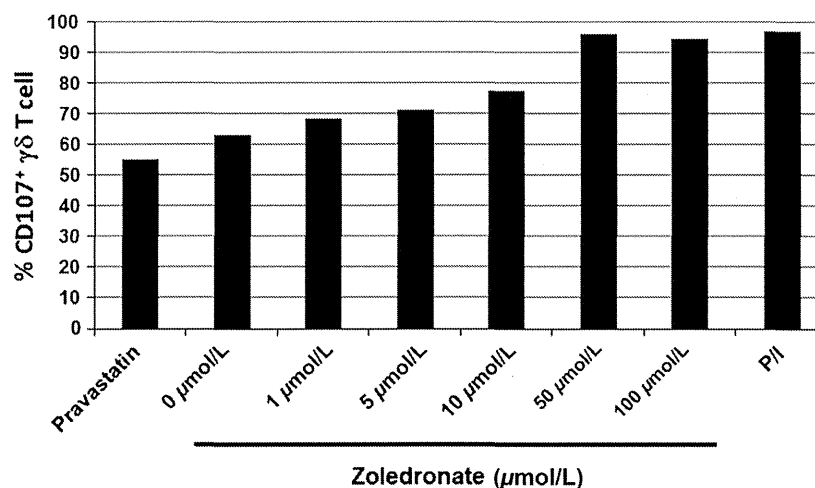


**Figure 2.** IPP accumulation by zoledronate was evaluated by the CD107 translocation assay of V $\gamma$ 9V $\delta$ 2 T-cells. Daudi cells were preincubated overnight with indicated concentration of zoledronate (0, 1, 5, 10, 50, and 100  $\mu$ mol/L) or 10  $\mu$ mol/L pravastatin sodium and used as stimulator cells. The  $5 \times 10^5$  Daudi cells were incubated with the same number of V $\gamma$ 9V $\delta$ 2 T-cells for 2 h at 37°C in the presence of GolgiStop and anti-CD107a/b mAbs. V $\gamma$ 9V $\delta$ 2 T-cells were also stimulated with PMA (20 ng/mL)/ionomycin (2  $\mu$ g/mL). CD107 translocation was measured by flow cytometry. Results were expressed as percentages of positive cells within the V $\gamma$ 9V $\delta$ 2 T-cell population.

infusions. After each i.p. injection, a large number of V $\gamma$ 9V $\delta$ 2 T cells was observed in the ascites (Fig. 3A); however, V $\gamma$ 9V $\delta$ 2 T cells were not increased in the blood (data not shown), suggesting that they did not enter the systemic circulation from the peritoneal cavity. The number of V $\gamma$ 9V $\delta$ 2 T-cells in ascites rapidly decreased within 7 days except in patient 2319.

It has been reported that zoledronate declines rapidly from the plasma with half-lives of 0.2 h [31]. By systemic injection of zoledronate, the concentration of zoledronate in the ascites might not be sufficient to block the mevalonate pathway and accumulate IPP in the tumor cells. Therefore, we compared the route of zoledronate injection, i.v. or i.p., preceded the infusion of V $\gamma$ 9V $\delta$ 2 T-cell administration. After i.v. zoledronate and i.p. V $\gamma$ 9V $\delta$ 2 T-cell injection, IFN- $\gamma$  production was detected in patient

2307 and 2328, but not in patients 2305, 2319, 2325, and 2336 (Fig. 3B). Importantly, the IFN- $\gamma$  production was observed when both zoledronate and V $\gamma$ 9V $\delta$ 2 T cells were i.p. injected. In patient 2334, i.v. zoledronate injection was omitted; she received three courses of i.p. zoledronate injection followed by i.p. V $\gamma$ 9V $\delta$ 2 T-cell injection. IFN- $\gamma$  was detected in the ascites with each V $\gamma$ 9V $\delta$ 2 T-cell injection.

Consistently, the concentration of zoledronate in the ascites fluid was higher and sustained longer after i.p. zoledronate injection than i.v. injection (Fig. S1). PBMCs from healthy donor were stimulated with indicated amount of zoledronate in AlyS203 medium containing 1000 IU/mL human recombinant IL-2 and 10% pooled human serum. Same donor derived PBMCs were cultured in IL-2 containing medium and in the presence of 10%

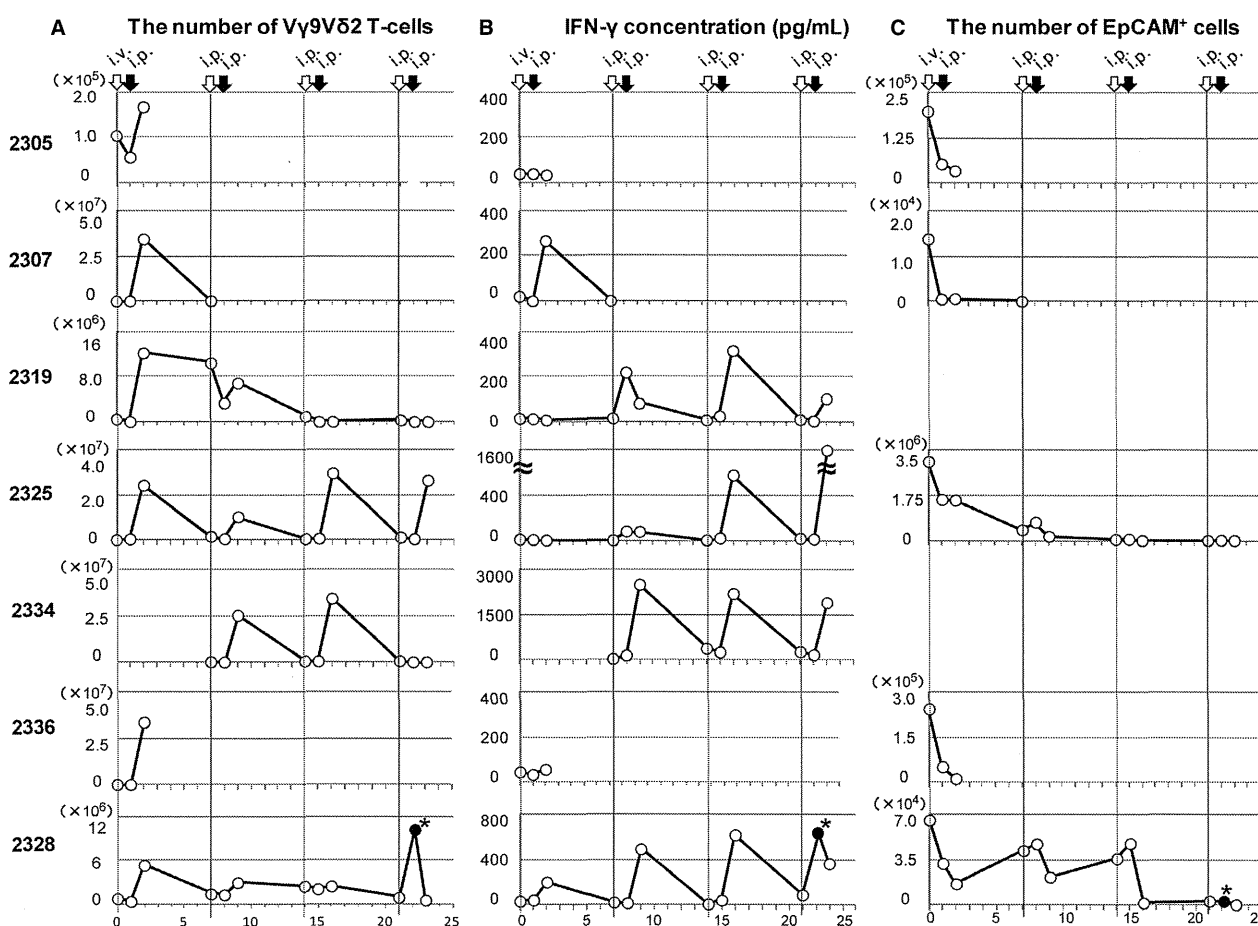


**Figure 3.** Dynamics of V $\gamma$ 9V $\delta$ 2 T cells and responses in patients with malignant ascites. (A) The number of V $\gamma$ 9V $\delta$ 2 T cells in ascites. The ascites fluid was drained from the peritoneal cavity via the indwelling catheter before zoledronate and V $\gamma$ 9V $\delta$ 2 T-cell injections and 24 h after V $\gamma$ 9V $\delta$ 2 T-cell injections. The cells were isolated by density gradient centrifugation and stained with anti-CD45, -CD3, and -TCRV $\gamma$ 9. The stained cells were analyzed on flow cytometry and the numbers of V $\gamma$ 9V $\delta$ 2 T cells calculated. (B) IFN- $\gamma$  concentration (pg/mL) in ascites at the indicated time points was measured by the FlowCytomix bead assay. (C) The cells from ascites were also stained with anti-EpCAM mAb and the numbers of EpCAM<sup>+</sup> tumor cells calculated. \*Sample was collected 4 h after i.p. V $\gamma$ 9V $\delta$ 2 T-cell injection.

patient ascites fluid for 14 days. The concentration of zoledronate was estimated by the expansion of V $\gamma$ 9V $\delta$ 2 T cells. While zoledronate was not detectable in the ascites harvested after i.v. zoledronate injection, the zoledronate concentration in the ascites peaked  $34.5 \pm 20$  nmol/L at 2 h, and rapidly declined to 10 nmol/L within 4 h after i.p. injection. The peak concentration reached higher and zoledronate concentration in the ascites sustained longer when zoledronate was i.p. injected than i.v. injected. These results indicated that local administration of zoledronate is important to sensitize tumor cells to V $\gamma$ 9V $\delta$ 2 T-cell recognition.

### The cytotoxicity of V $\gamma$ 9V $\delta$ 2 T cells

Because tumor cells from patients 2319 and 2334 were negative for EpCAM, it was difficult to calculate their precise tumor load. In the other five patients, the number of EpCAM<sup>+</sup> tumor cells in ascites fluid were significantly reduced after zoledronate and V $\gamma$ 9V $\delta$ 2 T-cell treatment (Fig. 3C). Immunofluorescence microscopy revealed that V $\gamma$ 9V $\delta$ 2 T cells attached to and surrounded EpCAM<sup>+</sup> tumor cells (Fig. 4A). These results are consistent with the cytological data (Fig. 4B). Large tumor cells and many leukocytes were present in the ascites. After V $\gamma$ 9V $\delta$ 2 T-cell injection, a large number of small mononuclear lymphocytes, presumably the V $\gamma$ 9V $\delta$ 2 T cells themselves, were observed in ascites. The number of large tumor cells was gradually reduced by the repetitive injections of V $\gamma$ 9V $\delta$ 2 T cells. In addition, many polymorphonuclear leukocytes were recruited into the ascites after zoledronate injection. The cytotoxic activity of V $\gamma$ 9V $\delta$ 2 T cells was also examined in vitro (Fig. 4D). When V $\gamma$ 9V $\delta$ 2 T cells from patient 2325 were cocultured with autologous EpCAM<sup>+</sup> tumor cells in vitro, V $\gamma$ 9V $\delta$ 2 T cells attached and killed tumor cells (movie clip S1). These results indicated that V $\gamma$ 9V $\delta$ 2 T cells indeed recognized tumor cells and exert antitumor activity.

### Clinical outcome

Clinical outcomes are summarized in Table 3. Patients 2305 and 2336 were withdrawn from the study after a single round of injections, due to disease progression. Patients 2307 and 2334 were withdrawn after one and three doses of V $\gamma$ 9V $\delta$ 2 T cells due to aspiration pneumonia and bacterial infection of the central venous catheter, respectively (although both patients experienced relief of their clinical symptoms and showed promising signs of immunological reactivity reflected by induction of IFN- $\gamma$  and the reduction of tumor cells in ascites). As shown in Figure 4C, bloody ascites of patient 2325 became clear after the treatment. In addition, the massive retention of

ascites was no longer present (Fig. 5A). Ascites was also reduced and almost disappeared in patient 2328 (Fig. 5B); therefore he received an additional two rounds of injections. Excellent palliation of symptoms was observed in these patients. However, the clinical benefits of i.p. V $\gamma$ 9V $\delta$ 2 T-cell injection were restricted to the local control of malignant ascites. Patients 2325 and 2328 developed mediastinal lymph node metastasis and bone metastasis, respectively.

### Adverse events

None of the patients experienced abdominal pain or any other toxicity related to i.p. injection of V $\gamma$ 9V $\delta$ 2 T cells. The most commonly observed treatment-related adverse events were fever (Grade 2:  $n = 3$ ) and zoledronate-induced hypocalcemia (Grade 3:  $n = 4$ ) (Tables 3 and S1). These events were generally mild-to-moderate in intensity and reversible. In contrast, most adverse events and symptoms were due to end-stage gastric cancer with peritoneal dissemination and disease progression, namely, loss of protein (Grade 2:  $n = 1$ , and Grade 3:  $n = 5$ ) and electrolyte disorders (Grade 3:  $n = 3$ , and Grade 4:  $n = 2$ ). Peritoneal dissemination caused serious complications, including intestinal obstruction and massive ascites, associated with weight loss, bloating, constipation, nausea, insomnia, and abdominal pain. Aspiration pneumonia (Grade 3) and disseminated intravascular coagulation (Grade 2) was observed in patients 2305 and 2319, respectively. Central venous catheter infection was detected in patients 2325 and 2334 (Grade 2). None of these adverse events was directly related to the administration of V $\gamma$ 9V $\delta$ 2 T cells and there were no treatment-related deaths.

### Discussion

We report here the direct evidence that adoptively transferred V $\gamma$ 9V $\delta$ 2 T cells do indeed recognize tumor cells and exert antitumor effector activity in vivo. Previously, we had conducted a clinical trial of adoptive V $\gamma$ 9V $\delta$ 2 T-cell transfer therapy for non-small cell lung cancer in patients who were refractory to other treatments [12, 13]. Autologous V $\gamma$ 9V $\delta$ 2 T-cells were expanded ex vivo using zoledronate and IL-2, and administered six times at 2-week intervals. The cultured cells were well-tolerated and some clinical benefit was observed in some patients in whom V $\gamma$ 9V $\delta$ 2 T cells were able to survive and expand [12, 13]. However, it remained to be determined whether transferred V $\gamma$ 9V $\delta$ 2 T cells infiltrated into the tumor and exerted antitumor effector functions in vivo. Therefore, we conducted a trial of adoptive V $\gamma$ 9V $\delta$ 2 T-cell therapy for patients with malignant ascites caused by advanced

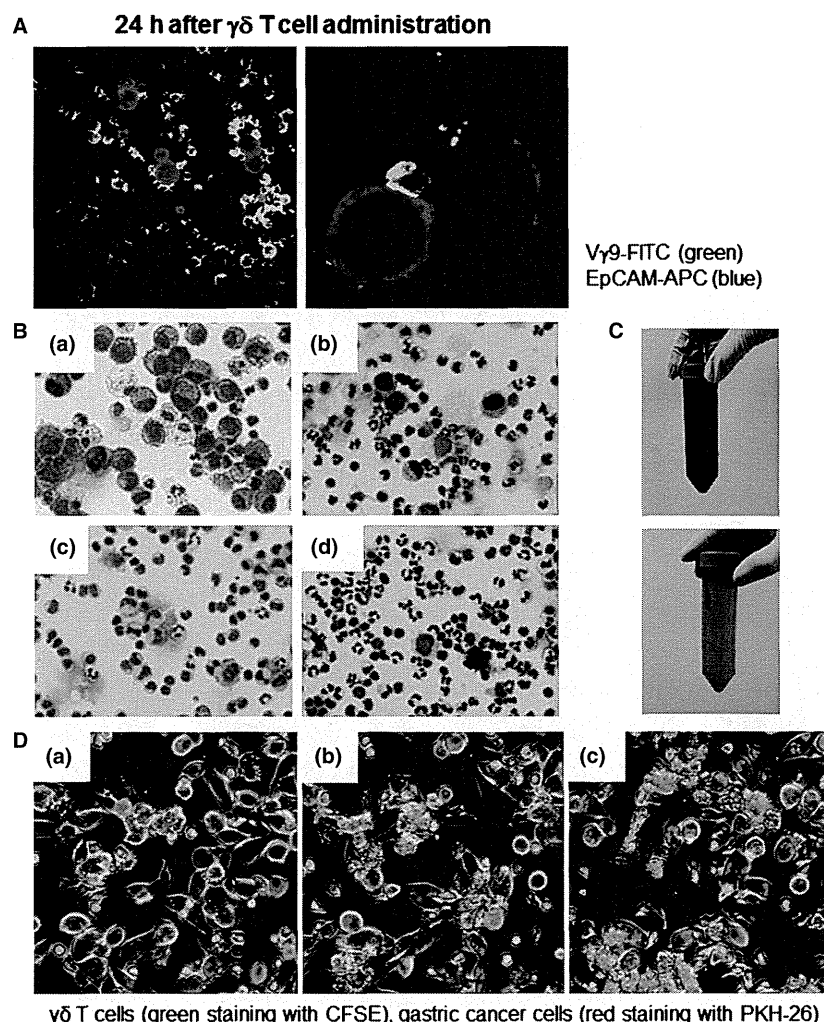


**Figure 4.** The cellular components and appearance of the ascites fluid. (A) The ascites fluid was harvested 24 h after V $\gamma$ 9V $\delta$ 2 T-cell injection; the cells were stained with anti-TCRV $\gamma$ 9-FITC and anti-EpCAM-APC mAbs and examined by confocal fluorescence microscopy. The EpCAM<sup>+</sup> tumor cells (blue) are attached to and surrounded by V $\gamma$ 9V $\delta$ 2 T cells (green) in ascites after V $\gamma$ 9V $\delta$ 2 T-cell injections. Magnification was 150 $\times$  on the left and 600 $\times$  on the right. (B) Smears were prepared, air-dried, and stained with Diff-Quik (Sysmex, Kobe, Japan) according to the manufacturer's instructions. Cell morphology was evaluated using bright field microscopy (OLYMPUS BX41 with Canon EOS Kiss X4 digital camera, OLYMPUS, Tokyo, Japan, magnification 200 $\times$ ). Data from patient 2328 on day 0 (a: before zoledronate i.v.), day 9 (b: 24 h after 2nd V $\gamma$ 9V $\delta$ 2 T-cell injection), day 21 (c: before zoledronate i.p.), and day 22 (d: 4 h after V $\gamma$ 9V $\delta$ 2 T-cell injection) are shown. (C) The appearance of ascites from patient 2325 before and after four courses of V $\gamma$ 9V $\delta$ 2 T-cell injections. (D)  $\gamma\delta$  T cells from patient 2325 (green staining with CFSE) recognized and killed autologous EpCAM<sup>+</sup> gastric cancer cells purified from ascites fluid (red staining with PKH-26), by direct contact. Tumor cells were attacked by the  $\gamma\delta$  T cells; collapse of the cell membranes led to apoptosis. It took approximately 2 h to progress from (a) to (c). Movie clip S1 is also provided.

gastric cancer. PBMC were harvested by apheresis; V $\gamma$ 9V $\delta$ 2 T cells were similarly prepared with zoledronate and IL-2; V $\gamma$ 9V $\delta$ 2 T cells were injected weekly into the peritoneal cavity, four times in total (Fig. 1B). Direct injection of V $\gamma$ 9V $\delta$ 2 T cells into the peritoneal cavity allows them direct access to the tumor cells, bypassing the difficulties of recruitment of transferred V $\gamma$ 9V $\delta$ 2 T-cells into solid tumors.

As shown in Figure 4A, many V $\gamma$ 9V $\delta$ 2 T cells attached to each EpCAM<sup>+</sup> tumor cell in the ascites 24 h after their

i.p. injection. Concomitantly, IFN- $\gamma$  was detected in ascites with kinetics similar to the increased number of V $\gamma$ 9V $\delta$ 2 T cells (Fig. 3B). The number of tumor cells in ascites was significantly reduced even after the first cell transfer and remained substantially lower during the course of the treatment (Fig. 3C). These results document tumor cell recognition and antitumor activity of V $\gamma$ 9V $\delta$ 2 T cells in vivo. When autologous tumor cells were isolated by anti-EpCAM magnetic beads and cocultured with autologous zoledronate-expanded V $\gamma$ 9V $\delta$ 2 T cells,

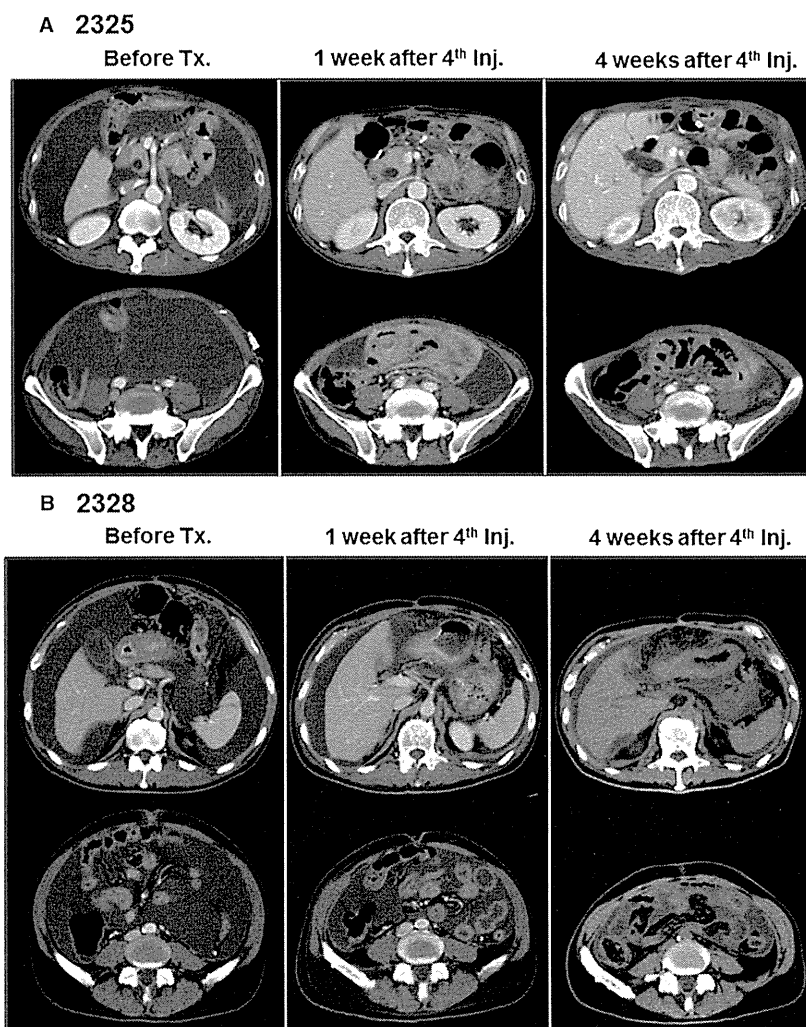


**Figure 5.** Computed tomography findings in patients 2325 (A) and 2328 (B). Retention of a large amount of ascites was observed before treatment (left panels). The amount of ascites was reduced 1 week (middle panels) and 4 weeks (right panels) after four courses of V $\gamma$ 9V $\delta$ 2 T-cell injections.

V $\gamma$ 9V $\delta$ 2 T cells indeed recognized and killed autologous tumor cells (Fig. 4D and movie clip S1). Such antitumor activity of i.p. V $\gamma$ 9V $\delta$ 2 T cells resulted in some remarkable clinical effects. While the appearance of ascites was initially bloody in patient 2325, it became clear after i.p. V $\gamma$ 9V $\delta$ 2 T-cell treatment (Fig. 4C). The reduction in ascites fluid was confirmed by computed tomography in patients 2325 and 2328 (Fig. 5). These results indicate that i.p. V $\gamma$ 9V $\delta$ 2 T-cell injection combined with zoledronate contributed to the local control of malignant ascites in some patients with gastric cancer for whom no standard therapy apart from paracentesis was available.

NBPs such as zoledronate are widely used in the clinic for the treatment of bone metastases and are known as potent stimulators of V $\gamma$ 9V $\delta$ 2 T cells [32]. Zoledronate blocks the mevalonate pathway, leading to intracellular

accumulation of IPP, its isomer dimethylallyl pyrophosphate (DMAPP) and ApppI [24, 33, 34]. Because V $\gamma$ 9V $\delta$ 2 T cells recognize these mevalonate metabolites in tumor cells, the high amounts of IPP and ApppI in zoledronate-treated tumor cells contributes to their recognition and lysis [35]. In the present study, zoledronate was administered 24 h prior to i.p. V $\gamma$ 9V $\delta$ 2 T-cell injection with the aim of presensitizing the tumor cells. We injected zoledronate either i.v. or i.p. and compared these routes of injection (Fig. 1B). As shown in Figure 3B, smaller amounts of IFN- $\gamma$  in ascites were detected in two of six patients after i.v. zoledronate injection, while higher amounts were found in ascites of all four patients who received i.p. zoledronate. These results are consistent with pharmacokinetic data for zoledronate, indicating that serum concentrations decline rapidly after infusion [31].

**Table 3.** Clinical outcome

| Patient ID | Numbers of $\gamma\delta$ |  | Clinical outcome |  |
|------------|---------------------------|--|------------------|--|
|            | T-cell injection          | Adverse events (Grade, CTCAE v. 4.0)   | Ascites          | Others   |
| 2305       | 1                         | Rectal obstruction (3) <sup>1</sup>  | No change        | Growth of primary lesion   |
| 2307       | 1                         | Aspiration (3) <sup>1</sup> , nausea (3), tumor pain (3), insomnia (2), hypoalbuminemia (2)  | No change        | Pleural effusion   |
| 2319       | 4                         | Fatigue (3), weight loss (3), hyponatremia (4), hypocalcemia (3), hypoalbuminemia (3), hypophosphatemia (3), female genital tract fistula (1), urinary tract infection (3), depressed level of consciousness (3), disseminated intravascular coagulation (2), lymphocyte count decreased (3) | No change        | Obstructive jaundice due to the growth of primary lesion                     |
| 2325       | 4                         | Fever (2), bloating (2), constipation (2), nausea (2), anemia (1), hypoalbuminemia (3), hypophosphatemia (3), hypocalcemia (3), urinary tract infection (2), insomnia (2), tumor pain (3), central venous catheter-related infection (2)   | Disappeared      | Mediastinal lymphadenopathy, pleural effusion, carcinomatous lymphangiosis   |
| 2334       | 3                         | Fever (2), nausea (2), insomnia (2), central venous catheter-related infection (2) <sup>1</sup> , tumor pain (3), anemia (3), hypocalcemia (3), hypoalbuminemia (3), palmar-plantar erythrodysesthesia syndrome (1)  | No change        | Metastasis to ovary  |
| 2336       | 1                         | Tumor pain (3), hypoalbuminemia (3), hypocalcemia (3), hyponatremia (3), hyperkalemia (4)  | No change        | Poor performance status <sup>1</sup> , metastasis to bladder, ovary and skin |
| 2328       | 4 (+2)                    | Fever (2), gastritis (2), constipation (2), hypoalbuminemia (3), lymphocyte count decreased (3)  | Reduced          | Bone metastasis  |

<sup>1</sup>Cause for discontinuance.

When we harvest ascites 2–8 h after i.p. zoledronate injection, ascites fluid contained the sufficient amount of zoledronate to expand V $\gamma$ 9V $\delta$ 2 T cell, suggesting they might inhibit farnesyl pyrophosphate (FPP) synthase activity in the tumor cells at this time point (Fig. S1). However, V $\gamma$ 9V $\delta$ 2 T cell did not respond to the ascites fluid harvested after i.v. zoledronate injection. Therefore, the zoledronate concentration in the ascites might not be sufficient for the inhibition of FPP synthase activity after i.v. administration. While the optimum dose and timing of zoledronate administration remain to be elucidated, the local administration of zoledronate is desired to inhibit FPP synthase and sensitize tumor cells in the abdominal cavity to efficient V $\gamma$ 9V $\delta$ 2 T-cells recognition.

In addition to the direct cytotoxic activity of V $\gamma$ 9V $\delta$ 2 T-cells on the tumor cells, their activation results in release of many cytokines and chemokines that may lead to the recruitment and activation of other immune cells. It has been reported that V $\gamma$ 9V $\delta$ 2 T cells induce dendritic cell maturation [36], B-cell activation [37], and polarization of Th1 immune responses [38]. We observed marked recruitment of neutrophils into the peritoneal cavity in this study (Fig. 4B); zoledronate alone induced granulocyte recruitment, suggesting that NBP induce  $\gamma\delta$  T cell-independent neutrophil recruitment in humans. Recently, Norton et al. [39] reported that intraperitoneal injection of alendronate, one of the FDA-approved NBPs, induced

peritoneal inflammation in mice. In their model, neutrophil recruitment depended on mast cells and IL-1R signaling. As mice lack the counterpart of human V $\gamma$ 9V $\delta$ 2 T cells and thus cannot respond to IPP and NBPs, the mechanism of peritoneal inflammation in mice might be different from our human study. Consistent with a previous reports that V $\gamma$ 9V $\delta$ 2 T-cell activation-induced neutrophil migration and increased their phagocytic potential and release of  $\alpha$ -defensins [40], and that  $\gamma\delta$  T cells rapidly induce CXCL8-mediated migration of neutrophils [41], infiltration of neutrophils was sustained after i.p. V $\gamma$ 9V $\delta$ 2 T-cell injection in this study (Fig. 4B). Despite the recruitment of many neutrophils into the peritoneal cavity, patients did not complain of abdominal pain and did not display any signs of peritonitis except retention of ascites after V $\gamma$ 9V $\delta$ 2 T-cell injection.

The combination of i.p. V $\gamma$ 9V $\delta$ 2 T-cell injection and zoledronate for the treatment of malignant ascites had acceptable tolerability without unexpected severe or long-lasting adverse events. Because patients with severe peritoneal dissemination and malignant ascites are generally in a poor condition, adverse events were frequent; many of them were not associated with cell transfer (Tables 3 and S1). However, pyrexia was probably associated with the release of proinflammatory cytokines induced by zoledronate and V $\gamma$ 9V $\delta$ 2 T-cell injection. The local i.p. injection of zoledronate and V $\gamma$ 9V $\delta$ 2 T cells might reduce the

systemic adverse events associated with the release of pro-inflammatory cytokines. Though the kinetics of IL-1 $\beta$ , IL-8, and TNF- $\alpha$  production in ascites fluid were similar with that of IFN- $\gamma$ , the changes of these cytokines were not detected in the patients' serum (data not shown). The IL-6 was elevated before the treatment in many of these advanced cancer patients, the changes associated with zoledronate and/or V $\gamma$ 9V $\delta$ 2 T-cells were not clear. The alterations in laboratory parameters were rarely considered clinically relevant to the treatment except for hypocalcemia caused by zoledronate.

The patients in this study received S-1 plus cisplatin, S-1 plus docetaxel, or docetaxel alone as a standard regimen for the treatment of unresectable or recurrent gastric cancer prior to the V $\gamma$ 9V $\delta$ 2 T-cell therapy (Table 1) [17, 18]. It has been reported that the overall median survival time in treatment-naïve patients with malignant ascites was approximately 5 months irrespective of the regimen received [16, 42, 43]. Once patients have become refractory to these chemotherapies, it is unlikely that they will experience a survival benefit from any treatment. In such cases, paracentesis and diuretics are primarily used in managing malignant ascites, neither of which is an anti-cancer treatment but solely palliative [15]. In contrast, the i.p. injection of V $\gamma$ 9V $\delta$ 2 T cells combined with zoledronate directly affects the tumor cells and reduces their number in the peritoneal cavity, as well as decreasing the amount of ascites fluid, leading to palliation of the symptoms of malignant ascites.

Although the i.p. V $\gamma$ 9V $\delta$ 2 T-cell injection and zoledronate treatment is unlikely to impact overall survival in such advanced disease, especially with metastasis, our results show a clear clinical benefit for the local control of malignant ascites (Fig. 5). We are planning to conduct a new clinical trial for treatment-naïve patients with peritoneal dissemination to evaluate the survival benefit of this treatment. Furthermore, combinations of this newly emerging therapy with established surgical, radiotherapy, and chemotherapy treatments are expected to improve the survival of cancer patients in future.

## Acknowledgements

This study was supported in part by a Grant-in-Aid for Scientific Research of the Ministry of Education, Culture, Sports, Science and Technology (K. K.). We thank Makoto Kondo, Takamichi Izumi, and Takuya Takahashi for performing the  $\gamma\delta$  T cell cultures; Nao Fujieda, Atsushi Kondo, Kaori Kanbara, and Ryuji Maekawa for immunological monitoring and laboratory assistance; Takashige Kondo, Yoko Yamashita, Tomoko Ishida, Haruka Matsushita, Yuki Nagasawa, Hiroki Yoshihara, and Akiko Fukuzawa for administrative supports.

## Conflict of Interest

Dr. Kazuhiro Kakimi received research support from Medinet Co. Ltd. (Yokohama, Japan). The costs of the entire  $\gamma\delta$  T cell culture production and part of the immunological assays were covered by Medinet Co. Ltd. The study sponsors had no involvement in study design; collection, analysis, and interpretation of data; writing the report; and the decision to submit the report for publication. All other authors have declared there are no financial conflicts of interest related to this work.

## References

- Hayday, A. C. 2000.  $\gamma\delta$  cells: a right time and a right place for a conserved third way of protection. *Annu. Rev. Immunol.* 18:975–1026.
- Carding, S. R., and P. J. Egan. 2002.  $\gamma\delta$  T cells: functional plasticity and heterogeneity. *Nat. Rev. Immunol.* 2:336–345.
- Triebel, F., and T. Hercend. 1989. Subpopulations of human peripheral T  $\gamma\delta$  lymphocytes. *Immunol. Today* 10:186–188.
- Bonneville, M., and E. Scotet. 2006. Human V $\gamma$ 9V $\delta$ 2 T cells: promising new leads for immunotherapy of infections and tumors. *Curr. Opin. Immunol.* 18:539–546.
- Riganti, C., M. Massaia, M. S. Davey, and M. Eberl. 2012. Human  $\gamma\delta$  T-cell responses in infection and immunotherapy: common mechanisms, common mediators? *Eur. J. Immunol.* 42:1668–1676.
- Wilhelm, M., V. Kunzmann, S. Eckstein, P. Reimer, F. Weissinger, T. Ruediger, et al. 2003.  $\gamma\delta$  T cells for immune therapy of patients with lymphoid malignancies. *Blood* 102:200–206.
- Dieli, F., D. Vermijlen, F. Fulfarò, N. Caccamo, S. Meraviglia, G. Cicero, et al. 2007. Targeting human  $\gamma\delta$  T cells with zoledronate and interleukin-2 for immunotherapy of hormone-refractory prostate cancer. *Cancer Res.* 67:7450–7457.
- Bennouna, J., E. Bompas, E. M. Neidhardt, F. Rolland, I. Philip, C. Galea, et al. 2008. Phase-I study of Innacell  $\gamma\delta$  T cells, an autologous cell-therapy product highly enriched in  $\gamma\delta$ 2 T lymphocytes, in combination with IL-2, in patients with metastatic renal cell carcinoma. *Cancer Immunol. Immunother.* 57:1599–1609.
- Kobayashi, H., Y. Tanaka, J. Yagi, N. Minato, and K. Tanabe. 2011. Phase I/II study of adoptive transfer of  $\gamma\delta$  T cells in combination with zoledronic acid and IL-2 to patients with advanced renal cell carcinoma. *Cancer Immunol. Immunother.* 60:1075–1084.
- Kondo, M., K. Sakuta, A. Noguchi, N. Ariyoshi, K. Sato, S. Sato, et al. 2008. Zoledronate facilitates large-scale ex vivo expansion of functional  $\gamma\delta$  T cells from

- cancer patients for use in adoptive immunotherapy. *Cytotherapy* 10:842–856.
11. Sato, K., M. Kondo, K. Sakuta, A. Hosoi, S. Noji, M. Sugiura, et al. 2009. Impact of culture medium on the expansion of T cells for immunotherapy. *Cytotherapy* 11:936–946.
  12. Nakajima, J., T. Murakawa, T. Fukami, S. Goto, T. Kaneko, Y. Yoshida, et al. 2010. A phase I study of adoptive immunotherapy for recurrent non-small-cell lung cancer patients with autologous  $\gamma\delta$  T cells. *Eur. J. Cardiothorac. Surg.* 37:1191–1197.
  13. Sakamoto, M., J. Nakajima, T. Murakawa, T. Fukami, Y. Yoshida, T. Murayama, et al. 2011. Adoptive immunotherapy for advanced non-small cell lung cancer using zoledronate-expanded gammadeltaTcells: a phase I clinical study. *J. Immunother.* 34:202–211.
  14. Dupont, J. B., Jr., J. R. Lee, G. R. Burton, and I. Cohn Jr.. 1978. Adenocarcinoma of the stomach: review of 1,497 cases. *Cancer* 41:941–947.
  15. Cavazzoni, E., W. Bugiantella, L. Graziosi, M. Franceschini, and A. Donini. 2013. Malignant ascites: pathophysiology and treatment. *Int. J. Clin. Oncol.* 18:1–9.
  16. Imamoto, H., K. Oba, J. Sakamoto, H. Iishi, H. Narahara, T. Yumiba, et al. 2011. Assessing clinical benefit response in the treatment of gastric malignant ascites with non-measurable lesions: a multicenter phase II trial of paclitaxel for malignant ascites secondary to advanced/recurrent gastric cancer. *Gastric Cancer* 14:81–90.
  17. Koizumi, W., H. Narahara, T. Hara, A. Takagane, T. Akiya, M. Takagi, et al. 2008. S-1 plus cisplatin versus S-1 alone for first-line treatment of advanced gastric cancer (SPIRITS trial): a phase III trial. *Lancet Oncol.* 9:215–221.
  18. Lenz, H. J., F. C. Lee, D. G. Haller, D. Singh, A. B. Benson III, D. Strumberg, et al. 2007. Extended safety and efficacy data on S-1 plus cisplatin in patients with untreated, advanced gastric carcinoma in a multicenter phase II study. *Cancer* 109:33–40.
  19. Ishigami, H., J. Kitayama, S. Kaisaki, A. Hidemura, M. Kato, K. Otani, et al. 2010. Phase II study of weekly intravenous and intraperitoneal paclitaxel combined with S-1 for advanced gastric cancer with peritoneal metastasis. *Ann. Oncol.* 21:67–70.
  20. Heiss, M. M., P. Murawa, P. Koralewski, E. Kutarska, O. O. Kolesnik, V. V. Ivanchenko, et al. 2010. The trifunctional antibody catumaxomab for the treatment of malignant ascites due to epithelial cancer: results of a prospective randomized phase II/III trial. *Int. J. Cancer* 127:2209–2221.
  21. Glimelius, B., K. Hoffman, U. Haglund, O. Nyren, and P. O. Sjoden. 1994. Initial or delayed chemotherapy with best supportive care in advanced gastric cancer. *Ann. Oncol.* 5:189–190.
  22. Pyrhonen, S., T. Kuitunen, P. Nyandoto, and M. Kouri. 1995. Randomised comparison of fluorouracil, epidoxorubicin and methotrexate (FEMTX) plus supportive care with supportive care alone in patients with non-resectable gastric cancer. *Br. J. Cancer* 71:587–591.
  23. Kang, J. H., S. I. Lee, D. H. Lim, K.-W. Park, S. Y. Oh, H.-C. Kwon, et al. 2012. Salvage chemotherapy for pretreated gastric cancer: a randomized phase III trial comparing chemotherapy plus best supportive care with best supportive care alone. *J. Clin. Oncol.* 30:1513–1518.
  24. Gober, H. J., M. Kistowska, L. Angman, P. Jenö, L. Mori, and G. De Libero. 2003. Human T cell receptor gammadelta cells recognize endogenous mevalonate metabolites in tumor cells. *J. Exp. Med.* 197:163–168.
  25. Clézardin, P. 2011. Bisphosphonates' antitumor activity: an unravelled side of a multifaceted drug class. *Bone* 48:71–79.
  26. Japanese Gastric Cancer Association. 2011. Japanese classification of gastric carcinoma: 3rd English edition. *Gastric Cancer* 14:101–112.
  27. Kondo, M., T. Izumi, N. Fujieda, A. Kondo, T. Morishita, H. Matsushita, et al. 2011. Expansion of human peripheral blood gammadelta T cells using zoledronate. *J. Vis. Exp.* e3182, doi: 10.3791/3182.
  28. Izumi, T., M. Kondo, T. Takahashi, N. Fujieda, A. Kondo, N. Tamura, et al. 2013. Ex vivo characterization of gammadelta T-cell repertoire in patients after adoptive transfer of Vgamma9Vdelta2 T cells expressing the interleukin-2 receptor beta-chain and the common gamma-chain. *Cytotherapy* 15:481–491.
  29. Fischer, K., R. Andreesen, and A. Mackensen. 2002. An improved flow cytometric assay for the determination of cytotoxic T lymphocyte activity. *J. Immunol. Methods* 259:159–169.
  30. Idrees, A. S. M., T. Sugie, C. Inoue, K. Murata-Hirai, H. Okamura, C. T. Morita, et al. 2013. Comparison of  $\gamma\delta$  T cell responses and farnesyl diphosphate synthase inhibition in tumor cells pretreated with zoledronic acid. *Cancer Sci.* 104:536–542.
  31. Chen, T., J. Berenson, R. Vescio, R. Swift, A. Gilchick, S. Goodin, et al. 2002. Pharmacokinetics and pharmacodynamics of zoledronic acid in cancer patients with bone metastases. *J. Clin. Pharmacol.* 42:1228–1236.
  32. Kunzmann, V., E. Bauer, J. Feurle, F. Weissinger, H. P. Tony, and M. Wilhelm. 2000. Stimulation of gammadelta T cells by aminobisphosphonates and induction of antiplasma cell activity in multiple myeloma. *Blood* 96:384–392.
  33. Roelofs, A. J., M. Jauhiainen, H. Monkkinen, M. J. Rogers, J. Monkkinen, and K. Thompson. 2009. Peripheral blood monocytes are responsible for gammadelta T cell activation induced by zoledronic acid through accumulation of IPP/DMAPP. *Br. J. Haematol.* 144:245–250.
  34. Monkkinen, H., S. Auriola, P. Lehenkari, M. Kellinsalmi, I. E. Hassinen, J. Vepsäläinen, et al. 2006. A new

- endogenous ATP analog (ApppI) inhibits the mitochondrial adenine nucleotide translocase (ANT) and is responsible for the apoptosis induced by nitrogen-containing bisphosphonates. *Br. J. Pharmacol.* 147:437–445.
35. Benzaid, I., H. Monkkonen, V. Stresing, E. Bonnelye, J. Green, J. Monkkonen, et al. 2011. High phosphoantigen levels in bisphosphonate-treated human breast tumors promote V $\gamma$ 9V $\delta$ 2 T-cell chemotaxis and cytotoxicity in vivo. *Cancer Res.* 71:4562–4572.
  36. Ismaili, J., V. Orlislagers, R. Poupot, J. J. Fournie, and M. Goldman. 2002. Human gamma delta T cells induce dendritic cell maturation. *Clin. Immunol.* 103:296–302.
  37. Brandes, M., K. Willimann, A. B. Lang, K. H. Nam, C. Jin, M. B. Brenner, et al. 2003. Flexible migration program regulates gamma delta T-cell involvement in humoral immunity. *Blood* 102:3693–3701.
  38. Poccia, F., M. L. Gougeon, C. Agrati, C. Montesano, F. Martini, C. D. Pauza, et al. 2002. Innate T-cell immunity in HIV infection: the role of V $\gamma$ 9V $\delta$ 2 T lymphocytes. *Curr. Mol. Med.* 2:769–781.
  39. Norton, J. T., T. Hayashi, B. Crain, J. S. Cho, L. S. Miller, M. Corr, et al. 2012. Cutting edge: nitrogen bisphosphonate-induced inflammation is dependent upon mast cells and IL-1. *J. Immunol.* 188:2977–2980.
  40. Agrati, C., E. Cimini, A. Sacchi, V. Bordoni, C. Gioia, R. Casetti, et al. 2009. Activated V $\gamma$ 9V $\delta$ 2 T cells trigger granulocyte functions via MCP-2 release. *J. Immunol.* 182:522–529.
  41. Caccamo, N., C. La Mendola, V. Orlando, S. Meraviglia, M. Todaro, G. Stassi, et al. 2011. Differentiation, phenotype, and function of interleukin-17-producing human V $\gamma$ 9V $\delta$ 2 T cells. *Blood* 118:129–138.
  42. Yamao, T., Y. Shimada, K. Shirao, A. Ohtsu, N. Ikeda, I. Hyodo, et al. 2004. Phase II study of sequential methotrexate and 5-fluorouracil chemotherapy against peritoneally disseminated gastric cancer with malignant ascites: a report from the Gastrointestinal Oncology Study Group of the Japan Clinical Oncology Group, JCOG 9603 Trial. *Jpn. J. Clin. Oncol.* 34:316–322.
  43. Oh, S. Y., H. C. Kwon, S. Lee, D. M. Lee, H. S. Yoo, S. H. Kim, et al. 2007. A phase II study of oxaliplatin with low-dose leucovorin and bolus and continuous infusion 5-fluorouracil (modified FOLFOX-4) for gastric cancer patients with malignant ascites. *Jpn. J. Clin. Oncol.* 37:930–935.

## Supporting Information

Additional Supporting Information may be found in the online version of this article:

**Figure S1.** The concentration of zoledronate was estimated by the V $\gamma$ 9V $\delta$ 2 T-cell bioassay. PBMCs from healthy donor were stimulated with indicated amount of zoledronate in AlyS203 medium containing 1000 IU/mL human recombinant IL-2 and 10% pooled human serum. After 14 day-culture, expansion of V $\gamma$ 9V $\delta$ 2 T cell was measured by flow cytometry to prepare the standard curve. Same donor-derived PBMCs were cultured in IL-2 containing medium and in the presence of 10% patient ascites fluid for 14 days. The concentration of zoledronate was estimated by the expansion of V $\gamma$ 9V $\delta$ 2 T cell using the standard curve.

**Movie clip S1.** Patient's V $\gamma$ 9V $\delta$ 2 T cells recognize and kill autologous tumor cells.

**Table S1.** Adverse events.

**Table S2.** % Cytotoxicity of V $\gamma$ 9V $\delta$ 2 T cells against Daudi cells w/o zoledronate treatment.

# Adoptive cytotoxic T lymphocyte therapy triggers a counter-regulatory immunosuppressive mechanism *via* recruitment of myeloid-derived suppressor cells

Akihiro Hosoi<sup>1,2</sup>, Hirokazu Matsushita<sup>1</sup>, Kanako Shimizu<sup>3</sup>, Shin-ichiro Fujii<sup>3</sup>, Satoshi Ueha<sup>4</sup>, Jun Abe<sup>4</sup>, Makoto Kurachi<sup>4</sup>, Ryuji Maekawa<sup>2</sup>, Kouji Matsushima<sup>4</sup> and Kazuhiro Kakimi<sup>1</sup>

<sup>1</sup> Department of Immunotherapeutics, The University of Tokyo Hospital, Tokyo, Japan

<sup>2</sup> MEDINET Co., Ltd. Yokohama, Japan

<sup>3</sup> Research Unit for Cellular Immunotherapy, The Institute of Physical and Chemical Research (RIKEN), Research Center for Allergy and Immunology (RCAI), Yokohama, Japan

<sup>4</sup> Department of Molecular Preventive Medicine, Graduate School of Medicine, The University of Tokyo, Tokyo, Japan

Complex interactions among multiple cell types contribute to the immunosuppressive milieu of the tumor microenvironment. Using a murine model of adoptive T-cell immunotherapy (ACT) for B16 melanoma, we investigated the impact of tumor infiltrating cells on this complex regulatory network in the tumor. Transgenic pmel-1-specific cytotoxic T lymphocytes (CTLs) were injected intravenously into tumor-bearing mice and could be detected in the tumor as early as on day 1, peaking on day 3. They produced IFN- $\gamma$ , exerted anti-tumor activity and inhibited tumor growth. However, CTL infiltration into the tumor was accompanied by the accumulation of large numbers of cells, the majority of which were CD11b<sup>+</sup>Gr1<sup>+</sup> myeloid-derived suppressor cells (MDSCs). Notably, CD11b<sup>+</sup>Gr1<sup>int</sup>Ly6G<sup>-</sup>Ly6C<sup>+</sup> monocytic MDSCs outnumbered the CTLs by day 5. They produced nitric oxide, arginase I and reactive oxygen species, and inhibited the proliferation of antigen-specific CD8<sup>+</sup> T cells. The anti-tumor activity of the adoptively-transferred CTLs and the accumulation of MDSCs both depended on IFN- $\gamma$  production on recognition of tumor antigens by the former. In CCR2<sup>-/-</sup> mice, monocytic MDSCs did not accumulate in the tumor, and inhibition of tumor growth by ACT was improved. Thus, ACT triggered counter-regulatory immunosuppressive mechanism *via* recruitment of MDSCs. Our results suggest that strategies to regulate the treatment-induced recruitment of these MDSCs would improve the efficacy of immunotherapy.

Adoptive T-cell immunotherapy (ACT) is recognized as a potent therapy for cancer.<sup>1,2</sup> Using gene transfer technologies, host T cells can be modified to stably express exogenous T-cell receptors (TCRs)<sup>3,4</sup> or chimeric antigen receptors (CARs)<sup>5-7</sup> that redirects their reactivity toward tumor-associated antigens. Many phase I and II clinical trials using tumor-infiltrating lymphocytes have now been conducted, as well some with

such genetically engineered T cells.<sup>1,8</sup> However, several crucial hurdles need to be overcome for the successful application of ACT. Tumors employ numerous different strategies to evade immune responses, including impaired antigen presentation, expression of ligands for negative costimulatory receptors on T cells (e.g. PD-L1, B7-H4), secretion of immunosuppressive factors (e.g. IL-10, TGF- $\beta$ , galectin-1, gangliosides, PGE2), ligands and factors for pro-apoptotic pathways (e.g. FasL, TRAIL, IDO) and induction of regulatory cell populations, such as CD4<sup>+</sup>CD25<sup>+</sup> regulatory T cells (Tregs), inducible Tr1 cells, IL-13-producing natural killer T (NKT) cells, and myeloid-derived suppressor cells (MDSC).<sup>9,10</sup> All these local events contribute to the establishment of a suppressive milieu in the tumor microenvironment which affects the anti-tumor activity of infiltrating immune cells. This results in a state of functional tolerance, defined as the coexistence of tumor-specific T cells and growing tumor cells.

To elicit efficient anti-tumor activities of transferred cytotoxic T lymphocytes (CTLs) and/or augmentation of their functions, further clarification of these tumor evasion strategies during ACT is required. Here, we investigated the intratumoral cellular immune response induced by the tumor-infiltrating adoptively-transferred CTLs using the B16-pmel-1 model.<sup>11,12</sup> We found that the anti-tumor activity of the infiltrating

**Key words:** CTL, MDSC, immunotherapy, adoptive transfer

**Abbreviations:** ACT: adoptive T cell immunotherapy; CTL: cytotoxic T lymphocyte; MDSC: myeloid-derived suppressor cell; DC: dendritic cell; Tregs: regulatory T cells; NKT: natural killer T; GM-CSF: granulocyte-macrophage colony stimulating factor  
Additional Supporting Information may be found in the online version of this article.

**Grant sponsor:** Grant-in-Aid for Scientific Research of the Ministry of Education, Culture, Sports, Science and Technology (to K.K.)

**DOI:** 10.1002/ijc.28506

**History:** Received 18 May 2013; Accepted 12 Sep 2013; Online 6 Oct 2013

**Correspondence to:** Kazuhiro Kakimi, Department of Immunotherapeutics, The University of Tokyo Hospital, 7-3-1 Hongo, Bunkyo-Ku, Tokyo 113-8655, Japan, Tel.: 81-35805-3161, Fax: 81-35805-3164, E-mail: kakimi@m.u-tokyo.ac.jp